AD-A068 224 NAVAL RESEARCH LAB WASHINGTON D C F/G 20/6
APPLICATION OF ADVANCED OPTICAL SPECTROSCOPIES TO THE STUDY OF --ETC(U)
APR 79 J M SCHNUR

UNCLASSIFIED NRL-MR-3974 NL

| OF |
ADA
068224

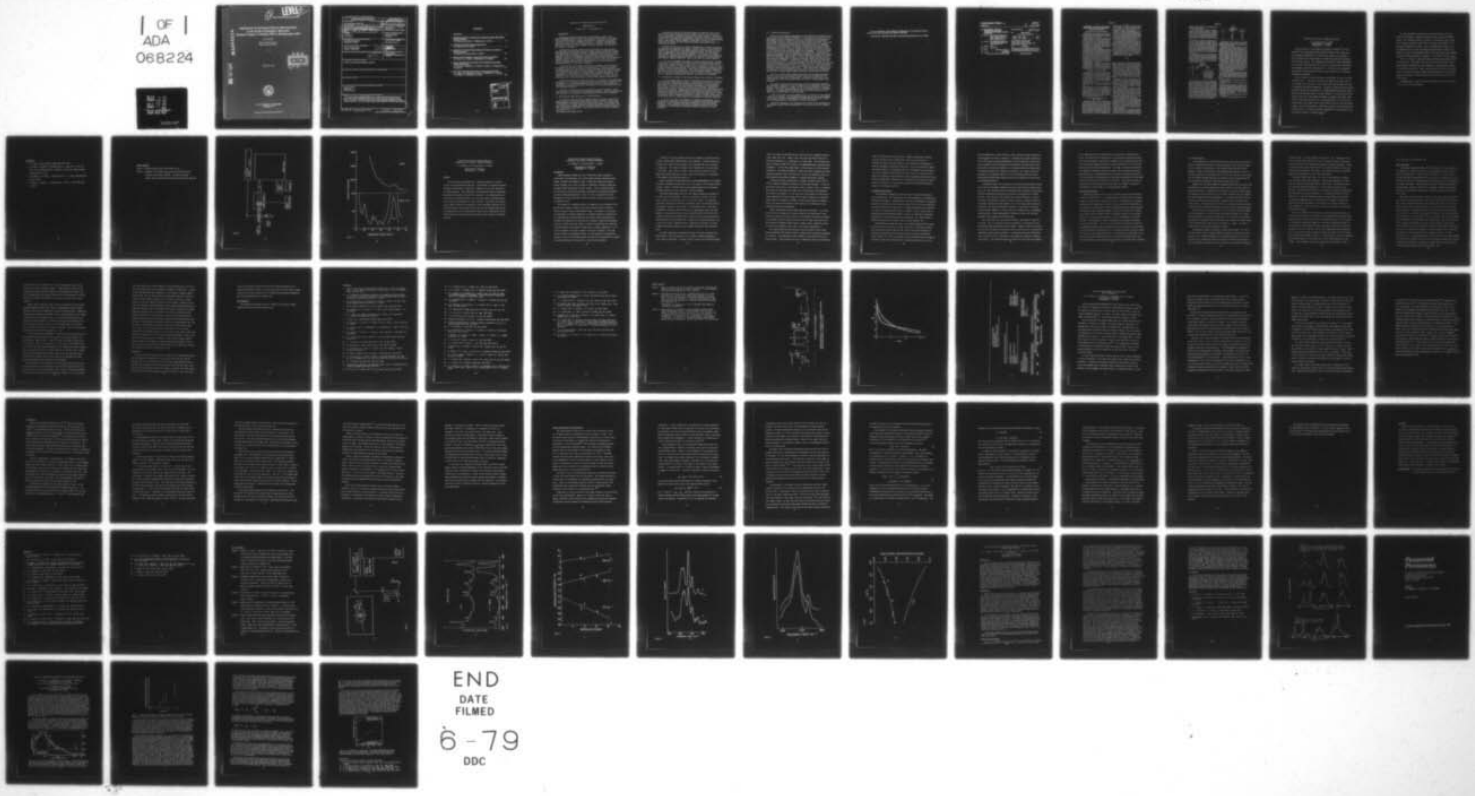

END
DATE
FILMED
6-79
DDC

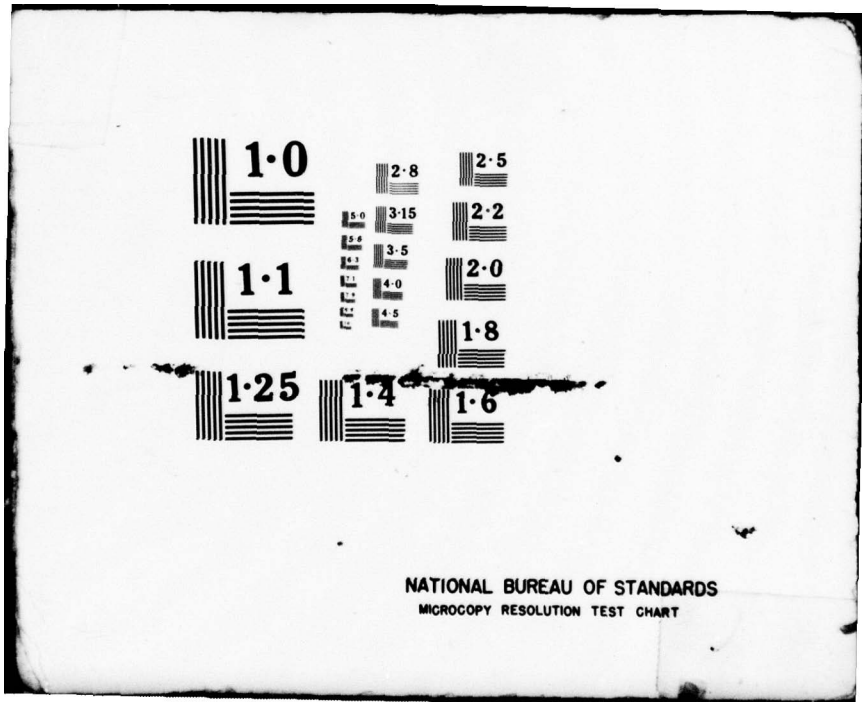
1·0
1·1
1·25
2·8
3·15
3·5
4·0
4·5
5·0
2·5
2·2
2·0
1·8
1·4
1·6
NATIONAL BUREAU OF STANDARDS
MICROCOPY RESOLUTION TEST CHART

NRL Memorandum Report 3974

Application of Advanced Optical Spectroscopies to the Study of Energetic Materials Summary Report 1 October 1977 to 30 September 1978

J. M. SCHNUR

Optical Techniques Branch
Optical Sciences Division

April 26, 1979

NAVAL RESEARCH LABORATORY
Washington, D.C.

SECURITY CLASSIFICATION OF THIS PAGE (When Data Entered)

REPORT DOCUMENTATION PAGE

READ INSTRUCTIONS BEFORE COMPLETING FORM

1. REPORT NUMBER: NRL Memorandum Report 3974	2. GOVT ACCESSION NO. (14)
3. RECIPIENT'S CATALOG NUMBER: NRL-MR-3974	
4. TITLE (and Subtitle): APPLICATION OF ADVANCED OPTICAL SPECTROSCOPIES TO THE STUDY OF ENERGETIC MATERIALS, SUMMARY REPORT, 1 OCT [illegible] 30 SEPTEMBER 1978	5. TYPE OF REPORT & PERIOD COVERED: Interim report on a continuing NRL problem.
	6. PERFORMING ORG. REPORT NUMBER
7. AUTHOR(s): J. M. Schnur	8. CONTRACT OR GRANT NUMBER(s): N00014-77WR80094, NR 122402
9. PERFORMING ORGANIZATION NAME AND ADDRESS: Naval Research Laboratory, Washington, DC 20375	10. PROGRAM ELEMENT, PROJECT, TASK AREA & WORK UNIT NUMBERS: NRL Problem C07-11A
11. CONTROLLING OFFICE NAME AND ADDRESS: Office of Naval Research, Arlington, Virginia 22217 (11) 26	12. REPORT DATE: Apr[illegible]79
	13. NUMBER OF PAGES: 72
14. MONITORING AGENCY NAME & ADDRESS(if different from Controlling Office): (12) 72p.	15. SECURITY CLASS. (of this report): UNCLASSIFIED
	15a. DECLASSIFICATION/DOWNGRADING SCHEDULE

16. DISTRIBUTION STATEMENT (of this Report)

Approved for public release; distribution unlimited.

17. DISTRIBUTION STATEMENT (of the abstract entered in Block 20, if different from Report)

18. SUPPLEMENTARY NOTES

19. KEY WORDS (Continue on reverse side if necessary and identify by block number)

Energetic materials
Spectroscopy
Optical techniques

20. ABSTRACT (Continue on reverse side if necessary and identify by block number)

This report contains a detailed description of the research performed during the past year under Contract N0014-77WR80094 Project Number 122402. This series of papers reflect the progress accomplished. This research program has been investigating the applicability of advanced optical techniques to the study of complex material problems associated with high energy substances.

DD FORM 1 JAN 73 1473 EDITION OF 1 NOV 65 IS OBSOLETE
S/N 0102-014-6601

251 950

SECURITY CLASSIFICATION OF THIS PAGE (When Data Entered)

CONTENTS

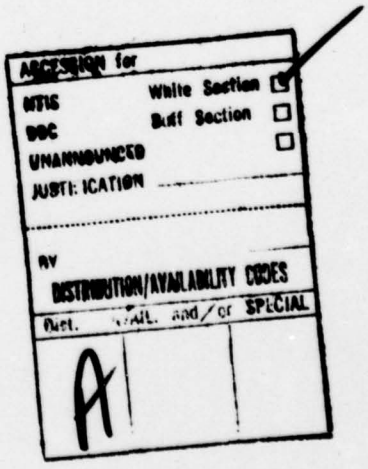

Application of Advanced Optical Spectroscopies

Summary Report

1 October 1977 - 30 September 1978

INTRODUCTION

This report describes the progress in ONR supported research under #N00014-78WR80094 Project #122402. The objective of the project is to demonstrate the applicability of Advanced Spectroscopic Techniques to problems of importance in the study of energetic materials. A variety of sophisticated optical approaches have been developed and used to determine the feasibility and utility of applying them to energetic material research. The work is in two principal task areas:

(a) High-pressure Raman and Brillouin spectroscopy are being applied to problems associated with binder failure in highly energetic propellant systems. The relationship of molecular structure to macroscopic properties such as the bulk modulii and the propensity for crack propagation is currently under investigation. Recently, a collaborative program has been initiated among the California Institute of Technology, University of Akron, Texas A&M, the Stanford Research Institute and the Naval Research Laboratory in order to study this problem comprehensively, and thus to determine its specific applicability to generating guidance for propellant formulation.

(b) Picosecond (10^{-12} second) spectroscopic techniques are being applied to the study of the primary events in the initiation of ultrafast reactions in energetic materials. By utilizing locally developed, state-of-the-art, ultrafast spectroscopic techniques it is now possible to observe the initial products; i.e. products formed within 10 picoseconds after the initial excitation. Such information can lead directly to a greater understanding of deflagration to detonation transitions (DDT) and can provide insights into the role, that additives can play in either sensitizing or desensitizing energetic formulations.

An anticipated result of this project will be the transfer of the appropriate technologies to those systems laboratories which are specifically charged to study detonations. Once suitably developed and perfected by NRL, these picosecond spectroscopic techniques should prove invaluable in the characterization of ultrafast detonation processes.

The work in these task areas has proceeded in several directions, all of which have led to the discovery of intriguing information. Results are summarized below and specific publications resulting from this work follow the summary.

I. High Pressure Raman Spectroscopy of Chain Molecules.

A. The study of the effects of pressure from 2 to 20 kilobars upon conformational order in short chain alkane fluids has been completed. Results from this experiment conclusively prove that short alkanes (i.e. less than or equal to 16 carbons in the chain) become more globular as pressure is increased. The most recent results suggest that for long chain alkanes the opposite occurs, i.e. that long alkanes (> 40 carbons in the chain) become more rod-like as pressure is increased above 5 kb.

Note: Manuscript submitted January 26, 1979.

The unexpected results for the short alkanes may shed some light upon recent results from viscoelastic studies designed to evaluate the use of fatty acids as surfactants to minimize friction between metal surfaces. Researchers at both Battelle Laboratories and Rensselaer Polytechnic Institute have reported recently that these additives unexpectedly increased the wear in some experiments. Some of these results could be readily interpreted on the basis of the discovery that alkane and chain become more gauche under applied stress, i.e. become more ball-like.

The other NRL observation of chain straightening as a function of pressure in long alkanes is especially intriguing. Previous studies of polyethylene have indicated that polyethylene, when either annealed at high pressures of crystallized at high pressure, will form highly extended chains. The observation of chain straightening at high pressures suggests that there may be an ordered liquid phase, accessible only at high pressures. This suggests that formulation techniques at higher pressures may provide a new approach to the generation of high strength, polymeric materials. Work in this area is currently underway.

B. In order to determine the length of pressure extended polymers via Raman spectroscopy we have invented under this project a new technique that utilizes a Fabry-Perot interferometer as a prefilter that is synchronized with the scan of a double monochromator. We have utilized this new technique to obtain very low frequency spectra of sharp fraction, very slowly crystallized polyethylene samples produced at Florida State University. These spectra have provided information about the length of the extended chain in the polyethylene samples. In FY 79 we will utilize this technique to study the role of pressure (in the diamond anvil cell) in determining conformational order in fluid and solid polyethylene.

II. Interferometric Studies of Viscoelastic Properties as a Function of Pressure.

A. We have demonstrated the utility of multipass interferometry to characterize unfilled polymer binder systems. During the next year we will study polymeric materials as a function of pressure and temperature by using Brillouin spectroscopy to determine the high frequency bulk modulus of these materials. This technique will allow the study of the effect of pressure, temperature, sample history, molecular weight, and polymer chemistry, upon these high frequency viscoelastic properties. Simultaneously, research groups at Stanford Research Institute and California Tech will characterize these same materials with respect to fracture resulting from the application of stress at ultrafast rates. It is expected that these collaborative efforts will provide a greater understanding of the molecular basis for crack formation and propagation in polymeric materials.

B. We will also apply the techniques of five-pass interferometry to the evaluation of viscoelastic properties of the alkanes and polyethylene materials previously studied by means of the Raman, diamond anvil cell spectroscopic techniques. This experiment should provide information about the role that intra-molecular order plays in affecting viscoelastic properties in chain molecules.

III. Picosecond Spectroscopy.

Last year we initiated an investigation of the utility of picosecond spectroscopy in the study of energetic materials. We have utilized the services of the Photochemistry Group at Georgetown University to provide us with the requisite photochemical and kinetic expertise and we have performed the experiments by utilizing NRL's state-of-the-art picosecond spectroscopic facilities. The initial phase of this collaborative NRL/Georgetown project has proven to be immensely successful in combining their synthetic and photochemical expertise with NRL's unique picosecond capabilities. We intend to proceed with the initial study of nitromethane as well as to initiate studies of other reactions where the application of ultrashort pulse technology should prove invaluable. The initial project in this area is the study of the photolysis of nitromethane. In spite of many years of investigation, numerous experimental approaches, and improvements in experimental techniques, both the qualitative and quantitative aspects of the photolysis of nitromethane remain unclear. A part of the confusion arises from the many conditions (temperature, irradiation wavelength, phase) under which the reactions have been conducted. Correlations of results from more than one laboratory, therefore, are poor. One group concludes from flash excitation that the primary photochemical act involves the formation of the aci-form which is converted thermally to formaldehyde and nitroxyl in a subsequent step. Other experiments indicated homolytic scission of the carbon-nitrogen bond to form methyl and nitro radicals in the primary photochemical step. Other photochemical studies led to the condlusion that nitromethane vapors irradiated at 313 nm yield formaldehyde from the excited singlet state and methyl and nitro radicals from the triplet.

While all of these results suggest mechanisms, none involves measurements taken on a time scale short enough to observe directly the formation of the initial products from excited nitromethane: microsecond flashes cannot yield definitive conclusions for processes that occur within a few nanoseconds after excitation.

The initial results from the picosecond resolution experiment demonstrate that significant quantities of $\cdot NO_2$ are present at ten nanoseconds, but not much earlier, after irradiation, by light, of neat liquid nitromethane at room temperature. This delay time eliminates the excited singlet state as the immediate precursor. It suggests either a triplet state of an isomer (such as the aci form) as the initial product of the photolysis.

In FY 79 the effect of various additives upon the kinetics of the formation of NO_2 will be studied. Such information may well lead to better understanding of the shock to detonation experiments in nitromethane and the effect of additives in determining the time required for shock to detonation.

Another key experiment to be performed in FY 79 will be the observation of the methylene radical and the observation of its interactions in the condensed state.

Future experiments will include the comparison of the observed kinetics between shock and electronically induced reactions.

Publications resulting from some of the work described above now follows.

United States Patent [19]

Schnur et al.

[11] **4,097,317**

[45] **Jun. 27, 1978**

[54] **DESENSITIZING AGENT FOR COMPOSITIONS CONTAINING CRYSTALLINE HIGH-ENERGY NITRATES OR NITRITES**

[75] Inventors: **Joel M. Schnur**, Springfield, Va.; **Richard S. Miller**, Crofton, Md.; **James P. Sheridan**, Burke; **A. D. Britt**, Alexandria, both of Va.

[73] Assignee: **The United States of America as represented by the Secretary of the Navy**, Washington, D.C.

[21] Appl. No.: **781,278**

[22] Filed: **Mar. 25, 1977**

[51] **Int. Cl.**[2] **C06B 45/34; C06B 25/34; C06B 45/06**

[52] **U.S. Cl.** **149/7; 149/92; 149/18; 149/88; 149/19.92; 149/19.1; 149/46**

[58] **Field of Search** 149/19.1, 88, 18, 11, 149/92, 7, 19.9, 19.92

[56] **References Cited**

U.S. PATENT DOCUMENTS

3,108,916	10/1963	Coffe	149/11
3,138,496	6/1964	Monical	149/11
3,884,736	5/1975	Stack	149/92

Primary Examiner—Ronald H. Smith
Assistant Examiner—Sam Silverberg
Attorney, Agent, or Firm—R. S. Sciascia; Philip Schneider; Thomas McDonnell

[57] **ABSTRACT**

Increasing the stability of composite energetic compositions containing crystalline high-energy nitrates or nitrites by the inclusion of saligenin into the composition.

6 Claims, No Drawings

DESENSITIZING AGENT FOR COMPOSITIONS CONTAINING CRYSTALLINE HIGH-ENERGY NITRATES OR NITRITES

BACKGROUND OF THE INVENTION

This invention pertains generally to energetic gas producing compositions and in particularly to a desensitizer for composite energetic compositions with crystalline high-energy nitrates or nitrites.

Many solid propellants or explosive, catagorized as composites, comprise an oxidizer, a binder, and a number of other ingredients, e.g., metal fuels, catalysts, or age stabilizers. Crystalline high-energy nitrates or nitrites (CHEN) are often used as the oxidizer. Their cost is relatively low and their energy content is high. A major difficulty with these nitrates or nitrites is the ease with which they explode accidentially.

This property of energetic compositions is actually a matrix of factors. Sensitivity includes the reaction of the energetic compositions to mechanical shock, heat, pressure, friction or any other stress that can cause detonation. While an energetic composition can be more sensitive to one stress than another, such a conposition would detonate if any stress is severe enough. Desensitization is defined as the technique by which an explosive or propellant is rendered less reactive to these factors with a minimum of decrease in the other properties, e.g., specific impulse or age stability.

Desensitization is accomplished by the selection of certain materials for the binder and/or the inclusion of a desensitizing agent. The most widely used desensitizing binder material is certain microcrystalline waxes. Unfortunately, this type of wax is scarce and expensive.

SUMMARY OF THE INVENTION

It is, therefore, an object of this invention to provide a new desensitizer for explosive and propellant composition having crystalline high-energy nitrates or nitrites.

A further object of this invention is to provide a desensitizer which is capable of reducing the sensitivity of a large number of compositions having crystalline high-energy nitrates or nitrites without decreasing the energy of the composition.

Another object of this invention is to provide a desensitizing agent which is inexpensive and readily available.

These and other objects are achieved by coating the nitrate or nitrite crystals of a composite energetic composition with saligenin prior to compounding in an amount sufficient to provide a CHEN-to-saligenin weight from 1820:1 to 600:1 or by incorporating saligenin into the binder of a composite energetic composition in an amount sufficient to provide a nitrate-to-saligenin weight ratio from 182:1 to 45:1.

DETAILED DESCRIPTION OF THE INVENTION

The precise mechanism by which saligenin desensitize CHEN compositions is not known. It is postulated that the inclusion of saligenin increases the free-radical trapping of the binder. This conclusion is based on the observed correlation between the ability of known binders to trap free radicals and the effectiveness of that binder in desensitizing the composition. Other factors, such as lubrication, energy absorption, and shock absorption of the binder contribute to some degree to the desensitization of the composition. Although the precise mechanism of this invention can not at this moment be demonstrated, it can be demonstrated that the inclusion of saligenin in a CHEN composition improves significantly the stability of that composition.

Saligenin is suitable as a desensitizing agent for any propellant or explosive composition containing one or more crystalline high-energy nitrates. Examples of such materials are cyclotrimethylenetrinitramine (RDX), cyclotetramethylenetetranitramine (HMX), pentaerythritol tetranitrate (PETN), ammonium nitrate (AN), ditrinitroethylurea (DiTeU), and nitroguanidine.

Any wax or other binder material which has sufficient processability and viscoelasticity for propellant or explosive manufacture may be used with saligenin and sensitivity of the composition would be decreased. Exemplary of these materials are saturated alcohols with a molecular weight from 400 to 800, alkanes with a molecular weight from 400 to 800, saturated acids with a molecular weight from 350 to 750, saturated esters with a molecular weight of 350 to 750, mixtures of the foregoing, polyethylene, polyisoprene, polyureathane, unsaturated polyester resins crosslinked with styrene, vinyl polymers of the general formula:

$$CH_2=CH$$
$$\quad\quad|$$
$$\quad\quad y$$

wherein y may be H, Cl, or COOH, and other thermoplastic, thermosetting, and/or crosslinked polymers Specific examples of wax binders are octadecyl terephthalate, N-octadecyl, O-docosanyl carbamate, 12-hydroxystearic acid, N-octadecyl N'-docosanyl urea, N-phenyl O-docosanyl carbamate, octadecyl stearate, docosanyl terephthalate, octadecyl succinate, resorcinyl docosanoate, docosanyl, 2-dodicon-1-yl succinate, p-hydroxy ethyl terephthalate, and hexadecanyl carbamate. The commercially obtained waxes are mixtures of compounds whose molecular weight may go as high as 3000.

Since saligenin is relatively chemically inert, the use of saligenin does not present any compatability problems with other ingredients commonly included into propellant or explosive compositions. Examples of additional ingredients are fuels, e.g., alunimum, zirconium or boron, or age stabilizers, e.g., squalene, or antifoam agents, e.g., dimethyl silicone.

The amount of saligenin to be added to a CHEN composition depends on the method of addition. If saligenin is added directly to the crystals prior to compounding, the CHEN-to-salgenin weight ratio if from 1820:1 to 600:1 and preferably from 1150:1 to 760:1. But if the saligenin is added to the binder prior to compounding the CHEN-to-saligenin weight ratio is from 182:1 to 45:1 and preferably from 120:1 to 60:1.

Saligenin is added to the crystals by either dissolving saligenin in a suitable solvent, e.g., methylene chloride or benzene, admixing the crystals with the solution, and evaporating the solvent, or melting the saligenin and admixing the crystals with the molten material. After the addition, compounding the composite energetic composition proceeds in the usual manner with any of the accepted techniques.

Saligenin is added to a wax binder by either admixing both in a suitable solvent, e.g., methylene chloride and removing the solvent or melting both and mixing. After the addition of saligenin, compounding the composite

energetic composition is done in the usual manner with any of the accepted methods.

In order to demonstrate the utility of the present invention several composite explosives comprising RDX and a wax binder were tested. The test results as shown in Table 2. It is understood that these examples are given by way of demonstration and are not meant to limit this disclosure or the claims to follow in any manner.

Compositions 2-6 in Table 1 were prepared by melting the wax binder and saligenin together, mixing the two until a uniform distribution is obtained, admixing the treated wax with RDX by the hot slurry method at 85° for 3 hours, cooling, filtering, and drying the composition. In short, the compositions after the addition of saligenin were compounded in the method required for composition A3 explosives by the operating procedures of the U.S. Navy.

Compositions 7 and 8 in Table 1 were prepared by dissolving saligenin in methylene chloride, admixing the solution with RDX, evaporating methylene chloride, admixing the treated crystals with the wax binder by the hot slurry method at 85° C for 3 hours, cooling, filtering, and drying the composition.

TABLE 1

Ex. No.	COMPOSITIONS RDX wt. %	Saligenin wt. %	Binder (wt. %)
1	100		
2	91	1	500 mw Sat. Alcohol (8)
3	91	1	500 mw Sat. Acid (8)
4	91	1	$CH_3(CH_2)_{17}$—O—C—$(CH_2)_{16}CH_3$ (8)
5	91	1	500 mw Sat. Alkane (8)
6	91	2	500 mw Sat. Alkane (7)
7	91	0.1	500 mw Sat. Alkane (8.9)
8	91	0.5	500 mw Sat. Alkane (8.5)

The sensitivity of a composition was tested by the Model 12 Impact Method which comprises placing the energetic composition on flint paper which is resting on a flat steel anvil and allowing a flat 1¼ inch plunger, which is attached to a 2.5 kg weight, to drop upon the compound from a predetermined height. The sensitivity was then measured in terms of the height from which the dropping plunger initiated an explosion. Each composition of Table 1 was tested at least 30 times. A result given in Table 2 is the average of all tests conducted on a particular composition. Also given in Table 2 are the sensitivities of the compositions. without saligenin.

TABLE 2

Ex. No.	TEST RESULTS Height (cm) w/sal.	Height (cm) w/o sal.
1		22
2	58.1	54.2
3	58.6	54.2
4	63.2	52.4
5	58.1	49.3
6	58.1	49.3
7	63.0	49.3
8	43.0	49.3

The first point to note from Table 2 is that saligenin should be added in amounts specified previously. This is especially true when saligenin is incorporated by a direct addition onto the crystals.

As can be seen from Table 2, the addition of saligenin consistently provides a 10 to 20% improvement in the resistance of a composite CHEN composition to unwanted detonations. With such improvements, many waxes which are marginally effective from a safety viewpoint would be rendered substantially safe by the addition of saligenin. Consequently, many more waxes and other materials are now available as substitutes for the ever increasingly scarce microcrystalline waxes as binder materials. In addition, all composite energetic compositions with crystalline high-energy nitrates or nitrites are made more safe by the addition of saligenin.

Obviously many modifications and variations of the present invention are possible in light of the above teachings. It is therefore to be understood that within the scope of the appended clains the invention may be practiced otherwise than as specifically described.

What is claimed and desired to be secured by Letters Patent of the United States is:

1. In a method for desensitizing a composite energetic composition with high-energy nitrate or nitrite crystals the improvement which comprises coating said crystals, prior to compounding said composition with saligenin in a crystal-to-saligenin weight ratio from 1820:1 to 600:1.

2. The method of claim 1 wherein said weight ratio is from 1150:1 to 760:1.

3. The method of claim 1 wherein said weight ratio is from 910:1.

4. In a method for desensitizing a composite energetic composition comprising high-energy nitrate or nitrite crystals and a wax binder the improvement which comprises admixing saligenin with said wax binder prior to compounding said composition in an amount sufficient to provide in said composition a crystal-to-saligenin weight ratio from 182:1 to 45:1.

5. The method of claim 4 wherein said ratio is from 120:1 to 60:1.

6. The method of claim 4 wherein said ratio is 91:1.

* * * * *

Fabry-Perot Pre Filter for Raman Spectroscopy

P. E. Schoen and J. M. Schnur
Naval Research Laboratory
Washington, D. C. 20375

Current interest in low frequency excitations in polymers[1] and biopolymers[2] has raised anew the long standing problem of stray light rejection in Raman spectrometers.[3] We report here progress in an attempt to use a Fabry-Perot (FP) interferometer in tandem with a Spex double monochromator for high contrast. This combination has produced a useful improvement in contrast over the Spex alone, by a factor of about 200, while maintaining the throughput, about 50% of the Spex alone. The system was not optimum by any means and we describe results from an apparatus which is now undergoing considerable development.

For the initial trial the system was run essentially by hand. The setup is shown in Fig. 1. The FP was set between the sample and the Spex entrance slit, aligned on the Spex axis. A white light source was switched on so that it illuminated the FP/Spex combination. The Spex was advanced by one half wavenumber and then the FP was scanned till a maximum signal was detected, indicating the FP and Spex were tuned to the same frequency. At this point the white light was turned off, laser light was allowed to illuminate the sample, and a scaler counted detected photons for a predetermined time. At the end of the counting period the tuning of the FP was optimized, the white light was turned on again, and the cycle repeated. This manual procedure was quite tedious but as shown in Fig. 2 it produced noteworthy improvement in the visibility of the low frequency bands of the alkane $C_{94}H_{190}$.[4]

For this experiment low reflectivity mirrors were used in the FP to assure high throughput, although the finesse and the contrast were thereby reduced. The finesse was about 30, and with a free spectral range of about 35 cm^{-1} (mirror spacing was about 150 μm), this gave a FP bandpass ~1 cm^{-1}, matching the bandpass of the Spex. Since the transmission function of the FP repeated itself once every free spectral range the FSR was chosen to be large and to place the transmission maxima of the laser line at some frequency distant from spectral features of interest, i.e. the 28 cm^{-1} band in $C_{94}H_{190}$.

There are a number of improvements which obviously must be made in such a system as this. Switching of the laser and white light sources, FP and Spex frequency synchronization, data accumulation, and FP tuneup all should be controlled automatically. Higher contrast mirrors should be used and the choice of the best free spectral range should be explored. We are currently engaged in developing a system along these lines and will report on it in a future paper.

Acknowledgement: This work has been supported in part by a grant from the U.S. Office of Naval Research.

References

1. J. F. Rabolt and B. Fanconi, Polymer 18, 1258 (1977).

2. R. Faiman, G. Vergoten, Y. Maschetto and D. A. Long, Proc. of the 5th Intl. Conf. on Raman Spectros., Freiburg, E. Schulz ed. (Schulz Verlag, Freiburg 1976), p. 544.

3. W. Proffitt, L. M. Fraas, P. Cervenka, and S. P. S. Porto, Applied Optics 10, 531 (1971).

4. F. Khoury, B. Fanconi, J. D. Barnes and L. H. Bolz, J. Chem. Phys. 59, 11 (1973).

Figure Captions

Figure 1 - Fabry-Perot/Spex tandem spectrometer set up.

Figure 2 - Spectrum of the alkane $C_{94}H_{190}$ using the Spex double monochromator alone (upper spectrum). Spectrum of the same sample using the tandem Fabry-Perot/Spex system (lower spectrum).

Figure 1

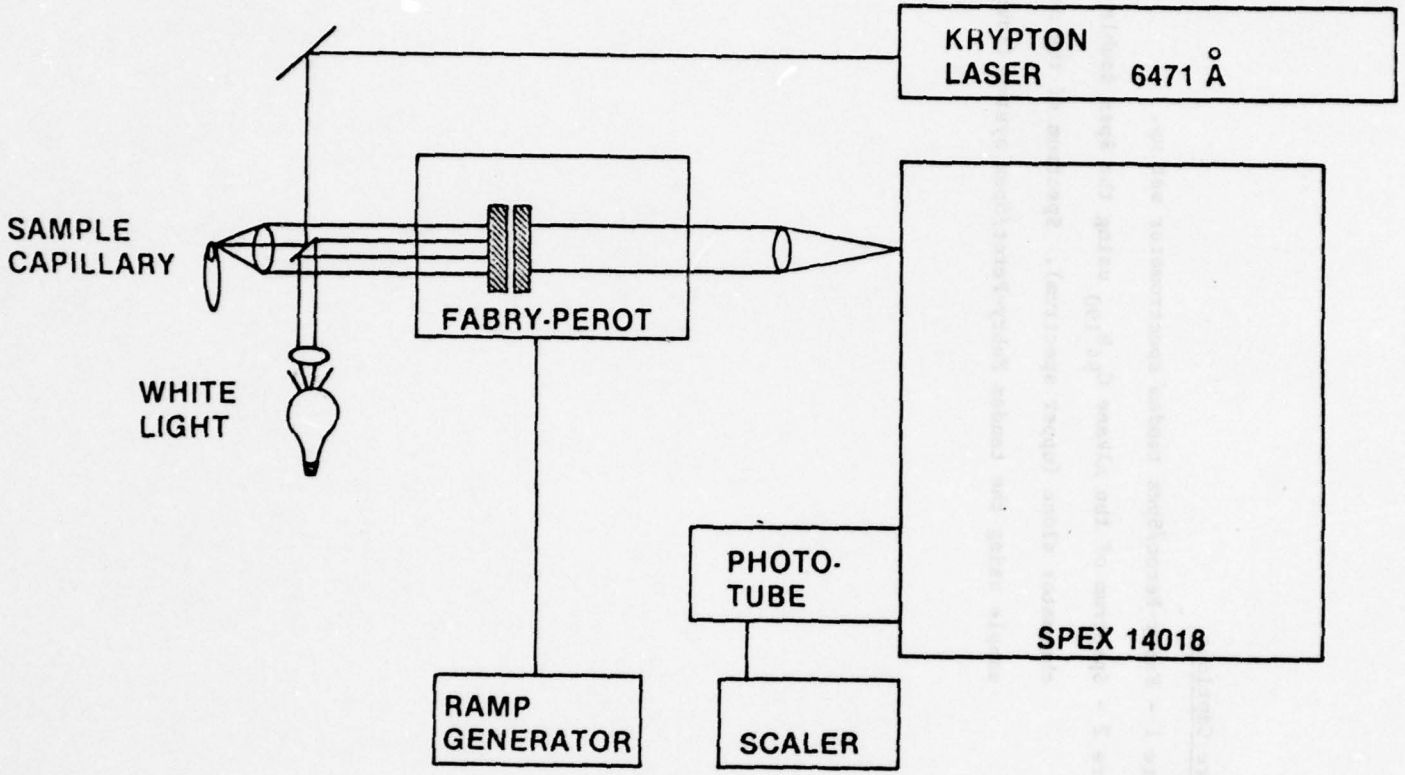
KRYPTON
LASER
6471 Å
SAMPLE
CAPILLARY
FABRY-PEROT
WHITE
LIGHT
PHOTO-
TUBE
SPEX 14018
RAMP
GENERATOR
SCALER

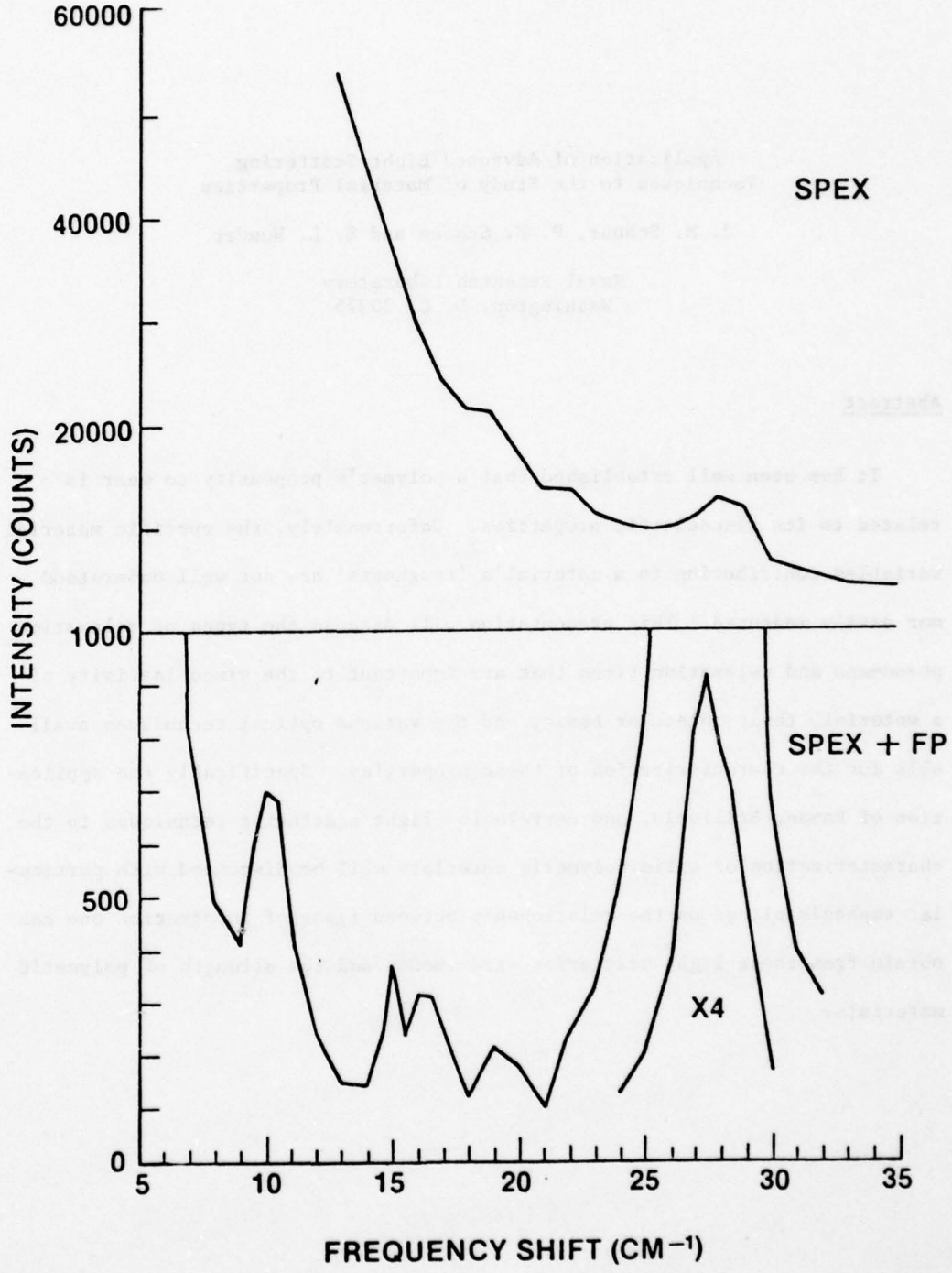
60000
40000
20000
1000
500
0
INTENSITY (COUNTS)
SPEX
SPEX + FP
X4
5
10
15
20
25
30
35
FREQUENCY SHIFT (CM⁻¹)

Figure 2

Application of Advanced Light Scattering Techniques to the Study of Material Properties

J. M. Schnur, P. E. Schoen and S. L. Wunder

Naval Research Laboratory
Washington, D. C. 20375

Abstract

It has been well established that a polymer's propensity to wear is related to its viscoelastic properties. Unfortunately, the specific material variables contributing to a material's 'toughness' are not well understood nor easily measured. This presentation will discuss the types of relaxation phenomena and relaxation times that are important to the viscoelastisity of a material, their molecular basis, and the various optical techniques available for the characterization of these properties. Specifically the application of Raman, Brillouin, and correlation light scattering techniques to the characterization of solid polymeric materials will be discussed with particular emphasis placed on the relationship between types of information one can obtain from these light scattering experiments and the strength of polymeric materials.

Application of Advanced Light Scattering Techniques to the Study of Material Properties

J. M. Schnur, P. E. Schoen and S. L. Wunder

Naval Research Laboratory
Washington, D. C. 20375

Introduction

Single component polymers can vary in molecular weight, dispersity, crystallinity and morphology, all of which affect material strength and wear. Indeed, a polymer can manifest a range of macroscopic properties (density, tensile strength, etc.) while its chemical composition, molecular weight and molecular weight distribution are kept constant. This is possible because the microscopic properties of molecular conformation and orientation profoundly affect macroscopic properties. Thus if we are to understand fully the mechanisms of strength and wear in polymers we must be able to probe them on the molecular level.

The response of a polymeric material is dependent on the frequency of the applied load, making it important in polymer characterization to measure material properties over a wide frequency range. Information on time scales not measurable by available techniques is typically obtained by making use of the time/temperature superposition principle (which implies equivalence of frequency and temperature for some systems): dynamical mechanical measurements made over a limited frequency range at a series of temperatures are converted to plots spanning a wide range of frequencies at a single temperature. It is clearly preferable to be able to measure a material's response in real time thereby avoiding the assumptions inherent in time-temperature superposition. Recently, progress has been made towards this goal with the application of light scattering techniques to the problem of polymer characterization.

Information about the internal dynamics of a polymer is obtained from the frequency changes light undergoes when it is scattered. A single frequency f_o of light from a laser strikes a sample and is scattered with a new frequency or frequencies. The change in frequency Δf is characteristic of some process in the sample. Thus Δf may be a doppler shift caused by reflection of the light from a moving particle, or else it may be the frequency of a sound wave in the sample or of a molecular vibration.

Light scattering can be divided under the broad subheadings of correlation, Brillouin, and Raman scattering according to the ranges of the frequency shifts involved. Figure 1 indicates the frequency ranges spanned and the molecular processes expected to occur within those frequency domains.

Correlation spectroscopy delas with the lowest frequencies detectable by the light scattering technique. The name, correlation, refers to the electronic technique of processing the detected optical signal. The resulting correlation function can be fourier transformed to give its frequency spectrum (the range is roughly 0.1 Hz to 1 MHz). As indicated in Fig. 1 this range corresponds to the slow, diffusive motions of large polymer chains and chain segments. The technique is used to observe the Brownian motion and rotation of polymer molecules in solution (light scattered from the moving particles is doppler shifted) and slow relaxations in solids near the glass transition, T_G. It also can be used to determine thermal conductivity, viscosity, and other transport properties through the local density fluctuations these processes cause.

At higher frequencies interferometric means can be used to measure frequency shifts. The lower frequency limit is about 1-10 MHz (depending on laser frequency stability). The upper limit is usually about 100 GHz although

there is no reason in principle why one could not work at frequencies several orders higher than this. Figure 1 shows that this range deals mainly with Brillouin scattering, i.e. scattering due to sound waves. The technique determines the elastic moduli (or in fluids, the compressibilities) governing sound propagation. In turn these moduli depend on high frequency collision-induced relaxations. In fluids the tumbling of smaller molecules, depending upon high frequency viscosity, falls into this range, as does the librational motion of small molecules and molecular segments in crystals and plastic crystals.

In Raman scattering, dealing with the highest frequency shifts, 10^{10} to 10^{14} Hz, spectral information is measured by diffraction grating. In this regime light scattering is a true molecular probe, as shown in Fig. 1, revealing the motions of atoms relative to each other, and sensitive to crystallinity and molecular conformation. In the lower end of this region are found the so called longitudinal "acoustic" modes (LAM's) whose frequencies are inversely proportional to the length of straight molecular chain segments in polymers. There is currently much interest in LAM's because of the information they yield about molecular conformations.

Optical measurements have the additional useful properties: (1) we can see the part of the sample that is being probed by the light beam, (2) the beam can be focused to a spot as small as a few microns if desired for looking at very small samples or regions of samples, and (3) light scattering can be done remotely on samples located inside of pressure cells, temperature baths, or even at great distances such as the tops of factory smokestacks...

The typical sample has many processes occurring within it which cause light scattering so that there is usually a great deal of information available in a spectrum. Interpretation of this information is the chief task of the spectroscopist. Light scattering is used in combination with X-ray diffraction,

neutron scattering, deuteration and other isotopic substitution, chemical labeling and substitution, computer modeling and other techniques to classify and identify spectral features seen in different circumstances in different compounds and classes of compounds. Since the discipline of light scattering is mature, a considerable library of information is now available that can be brought to bear upon new problems. The art of sorting out the details of a spectrum, drawing upon this pool of techniques and past work, has advanced considerably. Today there is the potential of utilizing this experience in the pursuit of a fuller understanding of the observed macroscopic properties of polymeric materials.

Correlation Spectroscopy

The correlation technique (1,2) has been used in light scattering for about fifteen years. The technique has had broad application to problems both biological and physical. Among the first uses were investigations of transport properties of fluids near their critical points (2,3,4), and of the diffusive motions (translational and rotational) of large macromolecules and viruses for the purpose of determining their sizes and shapes. (1,3,5) Another type of experiment has been measuring chemical reaction rate constants by observing fluctuations in the fluorescence of reacting species. (6) Liquid crystal dynamics and viscoelastic constants have also been observed. (1)

Correlation spectroscopy has been used to measure doppler shifts caused by blood flow in the arteries of living animals (7), to determine particle velocities in wind tunnels and jets (8), and to obtain the viscosities of lubricants by measuring the velocity with which a slug falls through the viscous liquid. (9) This last technique is quite new and extends the range of viscosities which can be measured by the falling slug method by one or two

orders of magnitude (to about 10^8 poise), while reducing the time required for the measurement from hours to minutes. To determine still higher viscosities (up to 10^{11} poise) correlation measurement of the distribution of fluid structural relaxation times (the diffusive "Mountain mode") has been shown to give good results in lubricants subjected to very high pressures and characterizes the dynamic viscosity over a range of frequencies. (10) Figure 2 shows the distribution of relaxation times for a pair of lubricants whose short time lubricating abilities differ sharply because of the difference in their short time relaxation behavior.

A substantial amount of the work done by correlation spectroscopy has been in the area of determining relaxation times for polymer chains in dilute solution. (11) The relaxation times for depolarized light scattered in the forward direction from polymer molecules were measured and extrapolated to infinite dilution. The relaxation times obtained were compared initially to the predictions of the Rouse-Zimm model and found in general to disagree except for the longest wavelength internal motions. (12) It was found, again contrary to prediction, that the local diffusive relaxation of fluctuations in position of small polymer segments in a large random coil resembled that of independent small molecules. Recent measurements by Caroline and Jones (13) show good agreement with an improved theoretical model.

All of the above cases have involved fluids or suspensions of particles in fluids. Use of a correlator with solid materials is rare because of the strong stray light scattering from such samples. However, recently the method has been used to measure low frequency motions in PMMA (14,15) as a function of temperature near the glass transition. Two relaxation times were observed of order .1 sec and .01 sec. The shorter time changed as a function of temperature below T_g. Its activation energy was found to be lower than that assigned

to the side-chain molecular reorientations from dielectric and NMR measurements. The internal motion observed from the correlation spectroscopy experiments was thus thought to arise from a coupling of this side-chain motion with the low activation energy process of torsional oscillations of the chain segments about their equilibrium positions. The longer relaxation time observed was temperature insensitive below T_g but merged with the backbone main chain relaxation at T_g. The measurements of this internal relaxation mode above T_g in the bulk phase by correlation spectroscopy agreed reasonably well with those obtained by mechanical and dielectric measurements. The relaxation below T_g, which has not been observed by other techniques, was thought to represent a rearrangement of free volume or of "configurational entropy."

Brillouin Spectroscopy

Brillouin spectroscopy (16) is light scattering caused by high frequency (10 MHz to 100 GHz) sound - i.e. random thermal oscillations which are always present in a sample with a non-zero temperature. The mechanism of scattering resembles that of Bragg X-ray diffraction, with a sound wave causing diffraction instead of crystal layers. As with Bragg scattering the scattering angle determines the sound wavelength observed, but since the sound wave is moving the scattered light is doppler shifted in frequency relative to the incident frequency. From the doppler frequency shift one can determine the velocity of sound. The absorption of sound is determined from frequency broadening of the scattered light. In turn one can then find the viscoelastic moduli of the sample and related transport properties, such as viscosity, thermal conductivity, and diffusion coefficients. (1,17) We note here that processes at such fast rates - on the nanosecond time scale - are difficult or impossible to obtain by ultrasonic methods and that X-ray and neutron techniques which do go to such frequencies are considerably less accurate and more difficult, expensive,

and sample-damaging.

A very large amount of work has been done on a wide variety of fluids and solids to determine their moduli, transport properties, and relaxation times. We will restrict our attention to a few examples chosen from the field of polymers. Energy in such systems is exchanged between molecular internal vibrations and external translational motions. (18) Processes which occur faster than such energy exchange encounter considerably different compressibilities and viscosities, for instance, than slower processes do. (1,19)

Paraffin oils have been examined in depolarized Brillouin scattering. (20) The tumbling of such chain molecules produces a spectral line whose width is related to viscosity. Linewidths were measured as a function of chain length and temperature and the values of the rotational relaxation time were compared with those obtained from flow birefringence. The values were similar but not identical, indicating a possible change in paraffin chain flexibility with longer chains. The relaxation times exhibited an Arrhenius temperature dependence and yielded rate-activation energies which had a chain length dependence.

Brillouin spectra have been obtained for poly (dimethyl siloxane) (PDMS) of molecular weight 7.7×10^4 and reveal four relaxation peaks in the hypersonic absorption as a function of temperature. (21) This data with microwave and dielectric relaxation times show Arrhenius type behavior for higher temperatures and WLF behavior below, with a sharp break at ~ 180°K. The authors suggest this to be the Debye temperature of PDMS.

The amorphous polymer poly (methyl acrylate) (PMA) appears to be one of the few solids in which a frequency dependent hypersonic relaxation has been observed. (22) Frequency dispersion in solid polymers often occurs at considerably lower frequencies than are encountered in Brillouin scattering so that the parameters obtained, such as the velocity, are generally the infinite

frequency values. For PMA the glass temperature is ~ 6°C. Relaxation is observed at temperatures above 85°C in both the hypersonic velocity and attenuation, and the size of the relaxation pehnomenon is frequency dependent. Using a single relaxation time theory the infinite frequency velocity and the relaxation time were determined. The value of the activation energy (7 Kcal/mole) suggests the relaxation is of the β type (side chain).

The Landau Placzek (LP) ratio - the ratio of the elastically scattered (zero frequency shift) light intensity to the Brillouin intensity - is often used as a probe of solid polymer behavior under stress. The Brillouin intensity should be relatively constant as it is an intrinsic property of the material. The elastic scattering on the other hand is sensitive to impurities, domain boundaries, strains, inclusions, etc. Mitchell and Guillet (23) and Coakley et al. (24) have studied the effects of annealing upon the LP ratio and they have suggested that as the temperature of a sample is dropped the naturally occurring fluctuations in the material are "frozen" in below the glass temperature. The LP ratio then is related to the amount of strain energy stored in the glass.

One of the difficulties of Brillouin scattering in amorphous solids is "contrast," the ability of the spectrometer to distinguish the Brillouin lines, which are weak, from the nearby elastic scattering peak, which is very strong. In recent years considerable progress has been made in improving contrast by the technique of multipassing (25) which increases contrast by many orders of magnitude. Dil et al. (26) and, very recently, Sandercock (27) have reported use of 5 and 7 pass systems to observe Brillouin scattering in metal surfaces. Since the penetration depth of light into a metal surface is small the technique yields elastic moduli for the region within a few hundred angstroms of the surface. Other phenomena such as the propagation of Lamm acoustic waves in

thick films also can be observed. (27)

Raman Scattering

In the Raman scattering process (28,29) the motion of an atom relative to its neighbors in a molecule or lattice causes fluctuations in the atomic or molecular polarizability. Since the first observation of the effect almost 50 years ago Raman spectroscopists have used a variety of techniques to try to determine the nature of the molecular motions which give rise to the Raman spectral lines they observe. This has involved the use of infrared spectroscopy, crystallography, symmetry, substitution of isotopes of different masses onto molecules, and calculations using computer models of molecules and molecular force fields.

One body of work of particular interest in the polymer field has been the application of Raman spectroscopy to the study of crystalline polymer morphology. Many polymers crystallize by folding their long chains into short segments which lie side by side like stacks of soda straws or sheaves of wheat, forming lamellae. The frequency shift of one of the bands of the Raman spectrum, the LAM, is a function of the lamellar thickness. Initial work was done on polyethylene and the n-paraffins. (30,31) The latter were used to determine the proportionality constant between the Raman frequency shift and the inverse of the straight chain length as a function of the number of carbon atoms. Frequency shifts obtained from polyethylene samples having lamellar morphology could then be correlated with lamellar thickness assuming that the Raman band corresponded to chain segments whose fold length was that of a similar n-paraffin. (31) For polyethylene single crystals where the tilt angle between the chains and the lamellar surface could be determined independently, lamellar thicknesses determined by the Raman method agreed fairly well with those obtained using small angle X-ray scattering (SAXS). (32)

Comparison has been more difficult for samples crystallized from the melt, since the tilt angle is generally unknown. Recent work has focused on the effects of the gauche (twisted) segments in the amorphous loop region (33), and of conformational (34) and mass defects (35) on the frequency of the LAM. This data has yielded information on the nature of the chain fold in polyethylene.

Despite initial difficulty, LAM's have now been observed in the helical polymers polyethylene oxide (36), isotactic polypropylene (37,38), polyoxymethylene (38) and in the copolymers (random) tetrafluoroethylene - hexafluoropropylene (39) and (block) polyethylene oxide - polypropyleneoxide (40), making it possible to use this Raman band in the study of the crystallization and structure of polymer lamellae. It should be noted that the advantage of the Raman scattering technique is that it does not depend (33) on the regularity of the lamellar stacking as is necessary for SAXS. This has permitted the observation of double lamellar populations. (32)

If the polymer chain is regarded as a uniform rod the proportionality constant between the LAM frequency and the inverse of the chain length is the sound velocity along the rod, $\nu = (E/\rho)^{1/2}$, where E is Young's modulus and ρ is the density. Thus, if an estimate of the tilt angle in the lamellar crystal is made, SAXS long period measurements can be combined with Raman frequency shifts to determine the ultimate Young's modulus of a polymer chain. Reports thus far (38,39) indicate that estimates made in this way agree with those determined from inelastic neutron scattering, but are substantially larger than those determined from wide angle X-ray scattering.

One particular class of problem which has received a great deal of theoretical attention for the past 30 years or so has been the mode structure of long chain molecules of the polyethylene type. (41,42) Considerable progress has been made in this effort and, of particular interest to us, not only have

the normal modes of the ideal straight chain been identified but also the effects upon the spectra of chain kinking have begun to be understood. In addition to the LAM's which give information on the length of straight segments between kinks, spectral features have been identified (see Fig. 3) which reveal the relative number of gauche and trans bonds (the "optical skeletal" bands) (43), and the ordering of chains and chain segments relative to each other (the "methylene stretching" bands (44) and crystal field splitting (45)). These bands have been used to investigate the effects of annealing on polymer lamellae thicknesses (46), the relative elastic moduli of crystalline and amorphous polymers (47), the effects upon chain order in model biological membrane chain molecules caused by phase changes and other perturbations (48), the effect of high pressure upon polymer structure and crystallinity (49), and the effect of high pressure upon chain kinking in the liquid alkanes. (50) In the latter case it has been seen that high pressure (up to 20 kbar) causes short chain alkanes (heptane, octane) to kink up and longer chains (polyethylene) to straighten out to the "super extended" chain phase. Work of this nature is continuing now to try to determine the relation between lubricant chain conformation and "lubricity," polymer structure and strength, and the influence upon these properties of perturbations such as temperature, pressure, chain length and dispersity, sample history, etc.

Conclusion

We have discussed briefly correlation, Brillouin, and Raman spectroscopies and have attempted to demonstrate in a general way their use and range of applicability. We have tried to show some of their unique abilities while at the same time emphasizing the need to employ them in concert with other spectroscopies and mathematical modeling techniques. We believe that light scattering is unusual and exciting because it is both new and old: new in the sense

of new and dramatically improved instrumentation and lengthening list of materials and fields in which it is finding use; and old in the sense of being a mature science with a great store of information and technology available to help with experimentation and interpretation.

Acknowledgement

We gratefully acknowledge the partial support of the Office of Naval Research for some of the work reported herein.

References

1. "Photon Correlation and Light Beating Spectroscopy," ed. by H.Z. Cummins and E. R. Pike, NATO Advanced Study Institute, Capri, Italy, 1978 (Plenum Press, New York 1974).

2. G. B. Benedek in "Polarization, Matière et Rayonnement, Livre de Jubilè en l'honneur du Professeur A. Kastler," ed. by the French Physical Society (Presses Universitaires de France, Paris 1969).

3. H. Z. Cummins and H. L. Swinney, and "Progress in Optics," ed. by E. Wolf (North-Holland, Amsterdam 1970) Vol. 8, p.133.

4. "Laser Light Scattering," by B. Chu (Academic Press, New York 1974).

5. H. Z. Cummins, P. D. Carlson, J. J. Herbert, and G. Woods, Biophys. J. 9, 518 (1969).

6. E. L. Elson and D. Magde, Biopolymers 13, 1 (1974); and D. Magde and E. L. Elson, Biopolymers 13, 29 (1974).

7. C. Riva, et al. Investigative Opthamology 11, 936 (1972).

8. A. D. Birch, D. R. Brown, J. R. Thomas, and E. R. Pike, J. Phys D (G.B.) 6, L71 (1973).

9. D. A. Jackson and D. S. Bedborough, to be published in J. Phys. D (G.B.) 11, L1 (1978).

10. P. W. Drake, J. F. Dill, C. J. Montrose, and R. Meister, J. Chem Phys. 67, 1969 (1977).

11. B. J. Berne and R. Pecora, "Dynamic Light Scattering," (Wiley, New York 1976) p.182.

12. W. I. Lee and J. M. Schurr, Chem. Phys. Lett. 23, 603 (1973).

13. D. Caroline and G. Jones, Bull. Am. Phys. Soc. 23, 272 (1978).

14. D. A. Jackson, E. R. Pike, J. G. Powles, and J. M. Vaughn, J. Phys. C (G.B.) 6, L55 (1973).

15. C. Cohen, V. Sankur, and C. J. Pings, J. Chem Phys. 67, 1436 (1977).

16. P. A. Fleury and J. P. Boon in "Advances in Chemical Physics," Vol. 24, ed. by I. Prigogine and S. A. Rice (John Wiley and Sons, New York 1973) p.1.

17. R. D. Mountain, Rev. Mod. Phys. 38, 205 (1966).

18. "Absorption and Dispersion of Ultrasonic Waves," by K. F. Herzfeld and T.A. Litovitz (Academic Press, New York 1959).

19. Q. H. Lao, P. E. Schoen, and B. Chu, J. Chem. Phys. 64, 3547 (1976).

20. J. V. Champion and D. A. Jackson, Mol. Phys. 31, 1159 (1976).

21. S. M. Lindsay, A. Adshead, and I. W. Shepherd, Polymer 18, 862 (1977).

22. Y. Y. Huang, E. A. Friedman, R. D. Andrews, and T. R. Hart in "Light Scattering in Solids," Proceedings of the International Conference in Paris, 1971 (Flammarion, Paris 1971) p.488.

23. R. S. Mitchell and J. E. Guillet, J. Polymer Sci.: Polymer Phys. ed. 12, 713 (1974).

24. R. W. Coakley, R. S. Mitchell, J. R. Stevens, and J. L. Hunt, J. App. Phys. 47, 4271 (1976).

25. J. R. Sandercock in "Light Scattering in Solids," ibid, ref. 22, p.9.

26. J. G. Dil and E. M. Brody, Phys. Rev. B14, 5218 (1976).

27. J. R. Sandercock, Bull. Am. Phys. Soc. 23, 387 (1978).

28. "Raman Spectroscopy," ed. by H. A. Szymanski (Plenum Press, New York 1967).

29. "Polymer Characterization - Interdisciplinary Approaches," ed. by C. D. Craver (Plenum Press, New York 1971).

30. R. F. Schaufele, J. Chem. Phys. 49, 4168 (1968).

31. W. L. Peticolas, G. W. Hibler, J. L. Lippert, A. Peterlin, H. Olf, Appl. Phys Letts. 8, 87 (1971).

32. J. Dlugosz, G. V. Fraser, D. Grubb, A. Keller, J. A. Odell, P. L. Goggin, Polymer 17, 471 (1976).

33. S. L. Hsu and S. Krimm, J. Appl. Phys. 48, 4018 (1977).

34. D. H. Reneker and B. Fanconi, J. Appl. Phys. 46, 4144 (1975).

35. B. Fanconi and J. Crissman, J. Polymer Sci., Polymer Letts. Ed. 13, 421 (1975).

36. A. Hartley, Y. K. Leung, C. Booth and I. W. Shepherd, Polymer 17, 355 (1976).

37. S. L. Hsu, S. Krimm, S. Krause, G. S. Y. Yeh, J. Polym. Sci., Polym. Lett. Ed. 14, 195 (1976).

38. J. F. Rabolt and B. Fanconi, J. Polym. Sci., Poly. Lett. Ed. 15, 121 (1977).

39. J. F. Rabolt and B. Fanconi, Polymer 18, 1258 (1977).

40. A. J. Hartley, Y. K. Leung, C. Booth, I. W. Shepherd, Proc. of the 5th Intl. Conf. on Raman Spect. (Schulz Verlag, Freiberg 1976) ed. by E. D. Schmid, p.496.

41. M. Tasumi and T. Shimanouchi, J. Mol. Spectros. 9, 261 (1962).

42. J. H. Schachtschneider and R. G. Snyder, Spectrochim. Acta 19, 85 (1963) and also 19, 117 (1963).

43. J. L. Lippert and W. L. Peticolas, Proc. Nat. Acad. Sci. 68, 1572 (1971).

44. K. Larsson, Chem. Phys. Lipids 10, 165 (1973); and K. Larsson and P. Rand, Biochim. Biophys. Acta 326, 245 (1973).

45. F. J. Boerio and J. L. Koenig, J. Chem. Phys. 52, 3425 (1970).

46. J. L. Koenig and D. L. Tabb, J. Macromol. Sci-Phys. B9, 141 (1974).

47. A Peterlin, H. G. Olf, W. L. Peticolas, G. W. Hibler, and J. L. Lippert, Polymer Lett. 9, 583 (1971).

48. B. P. Gaber and W. L. Peticolas, Biochim. Biophys. Acta 465, 260 (1977); R. G. Priest and J. P. Sheridan in "Liquid Crystals and Ordered Fluids," ed. by J. F. Johnson and R. S. Porter (Plenum Press, New York 1978) p.209; and J. P. Sheridan, J. M. Schnur and P. E. Schoen, Biochemistry, (to be published).

49. C. K. Wu and M. Nicol, J. Chem. Phys. 58, 5150 (1973); and Chem. Phys. Lett. 24, 395 (1974).

50. P. E. Schoen, R. G. Priest, J. P. Sheridan, and J. M. Schnur, Nature 270, 412 (1977).

Figure Captions

Figure 1 - Range of frequency shifts encountered in correlation, Brillouin and Raman spectroscopy and the excitation frequencies in various samples which these techniques may be used to measure.

Figure 2 - Correlation functions $\sigma(t)$ for a polyphenyl ether (O) at 1.2 kbar pressure and for a short chain methyl phenyl siloxane (Δ) at 2.1 kbar. The two curves illustrate relaxation functions for liquids which have the same low frequency, long time scale viscosity. The latter polymer will quickly relax a suddenly applied stress whereas the former will not.

(Permission of C. Montrose (ref. 10) to reproduce this figure is gratefully acknowledged.)

Figure 3 - Raman spectrum of the model biological membrane molecule, dipalmitoyl phosphatidyl choline, which shows many of the features typical of paraffin and polyethylene molecules. Each spectral band is labeled with the type of atomic motion causing it and the numbers give the frequency shifts in wavenumbers. (1 wavenumber = 3×10^{10} Hz). The LAM at 154 wavenumbers is fairly weak in this sample whereas in polyethylene and the n-paraffins it is quite strong.

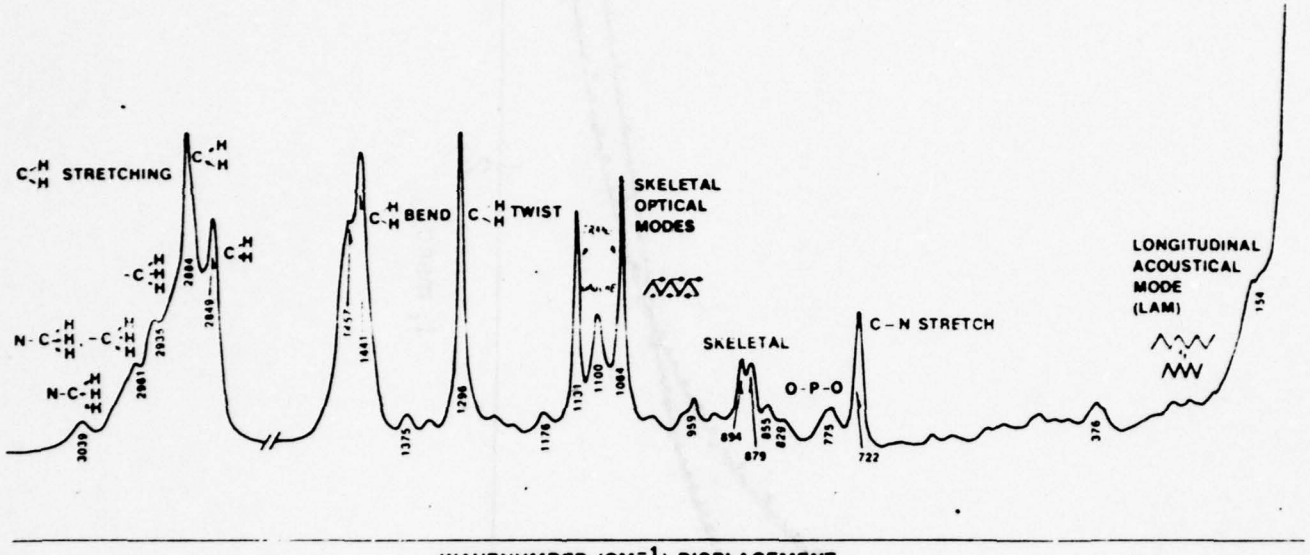

RAMAN SPECTRUM OF DIPALMITOYL PHOSPHATIDYL CHOLINE
(EXCITATION SOURCE; Kr LASER AT 647 nm)

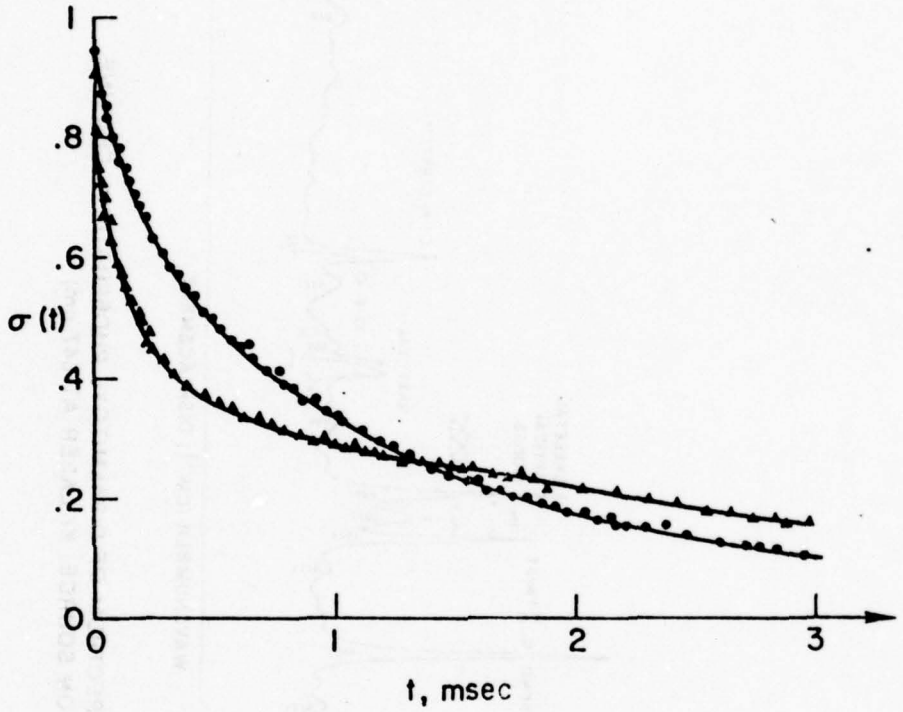
1
.8
.6
σ (t)
.4
.2
0
0
1
2
3
t, msec

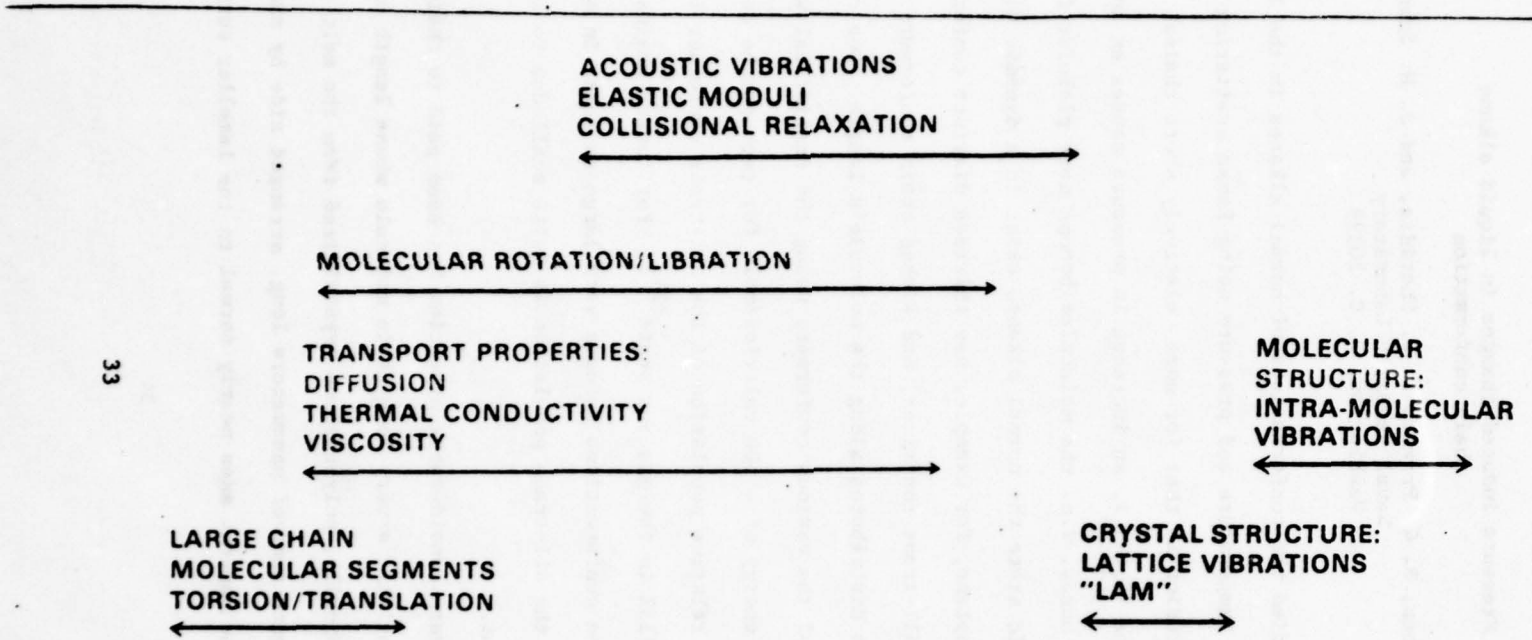
ACOUSTIC VIBRATIONS
ELASTIC MODULI
COLLISIONAL RELAXATION
MOLECULAR ROTATION/LIBRATION
TRANSPORT PROPERTIES:
DIFFUSION
THERMAL CONDUCTIVITY
VISCOSITY
MOLECULAR
STRUCTURE:
INTRA-MOLECULAR
VIBRATIONS
LARGE CHAIN
MOLECULAR SEGMENTS
TORSION/TRANSLATION
CRYSTAL STRUCTURE:
LATTICE VIBRATIONS
"LAM"
CORRELATION SPECTROSCOPY
INTERFEROMETRY
LIGHT BEATING SPECTROSCOPY
RAMAN SPECTROSCOPY
10^0 10^2 10^4 10^6 10^8 10^10 10^12 10^14
FREQUENCY SHIFT (Hz)

Pressure induced changes in liquid alkane chain conformation

P. E. Schoen, R. G. Priest, J. P. Sheridan, and J. M. Schnur
Naval Research Laboratory
Washington, D. C. 20375

We have studied the conformations of normal alkanes in the liquid state as a function of temperature and pressure using Raman scattering as a probe.[1] Our primary conclusion is that for some relatively short chains, at least as long as hexadecane ($C_{16}H_{34}$), an increase in pressure causes an increase in the number of gauche bonds, i.e. the molecules become more globular in shape.

In the liquid state the normal alkanes exist in a dynamic mixture of conformations. n-heptane, for example, has thirteen distinct conformers: the straight chain, all-trans conformer, and kinked chain conformers with up to four gauche bonds distributed along the molecule's length. One can calculate the populations of the various conformers using the statistical weight of each conformer and an energy of ~ 500 calories/mole for each gauche bond. For heptane (C_7H_{16}) the relative population of the all-trans conformer is small but easily detected (15% in the gaseous state[2]). For longer chains the number of possible gauche conformations becomes very large so that, in spite of its energy advantage the all-trans population is quite small due to its small statistical weight.

In recent years considerable attention has been paid to chain conformation in linear polyethylene, a very long chain molecule whose length can be several micrometers. Typically, polyethylene crystallized from the melt folds into trans chain segments tens of nanometers long, arranged side by side to form lamellae, with the segment axes nearly normal to the lamellar surface. On the

other hand when polyethylene is crystallized at high pressure, ~ 5 kbar, the chains are extended to their full lengths and there is evidence based on differential thermal analysis that in the high pressure liquid before crystallization the polyethylene chains exist in a "nematic"-like state, an ordered liquid phase.[3]

No such ordered liquid phase has been observed in the alkanes but the possibility of liquid crystalline-like effects in these shorter chain materials is of sufficient interest to justify studying in detail the chain morphology of the liquid alkanes as a function of pressure. Our procedure for alkane chains shorter than nonane has been to look for changes in the intensities of Raman bands associated with the populations of specific all-trans or gauche conformers. For the longer chains we have monitored Raman bands sensitive to trans or gauche bond populations rather than conformer populations.

Because of their obvious usefulness considerable effort has been undertaken in the past 30 years or more to identify conformationally sensitive Raman bands in alkyl chain molecules such as the linear alkanes, phospholipid molecules of biological importance, and polyethylene. In 1949 Mizushima and Shimonouchi[4] pointed out the disappearance of the Raman lines assigned to the gauche conformations when alkane samples are solidified. The molecules exist only in the all-transconformation in the solid state. A band associated with the all trans conformations in the so-called "longitudinal acoustic mode" (LAM) which is due to an accordian-like vibration of the fully extended chain along its length, with a frequency inversely proportional to the number of carbon atoms in the chain. Mizushima and Shimonouchi used the frequency of the LAM to calculate an elastic

modulus for extended chain alkane molecules. Of greater interest to us, they also noted that in the liquid state in contrast to the solid state there are many more bands present in the Raman spectrum due to the co-existence of several rotational isomers in the fluid. The LAM's, they point out, are intense in the liquid form of the shorter homologs (butane, pentane) but are not observed in liquid hexadecane, indicating that the extended chain form is abundant in the liquid state of the lower homologs but nearly absent for the longer chain liquids.

This effect was examined in some detail by Schaufele.[5] In the alkane liquids C_5H_{12} through C_8H_{18} he identified LAM's and neighboring bands which he assigned to rotational isomers having straight chain segments shorter than the fully extended chain. These segments were separated from each other by gauche bonds. These assignments were made with aid from the model calculations of Snyder[6] and from Schaufele's previous work with Shimanouchi.[7]

For liquid alkanes longer than octane Schaufele was unable to detect a LAM. Recently, however, Snyder, et al.[8] were able to establish that very weak LAM bands can be detected in longer chains liquids up to $C_{20}H_{42}$. Unfortunately these band intensities are too low for our purposes. In any case, for the liquids up to octane one can measure changes in acoustic band intensities as a function of pressure and determine from them changes in trans and gauche conformer populations.

For longer chains an alternative Raman probe of conformation is the triplet of bands between 1000 and 1200 cm^{-1} called the optical skeletal bands (OS). Lippert and Peticolas[9] in 1971, with the help of model calculations

by Tasumi et al.[10] and by Snyder and Schachtachneider,[11] assigned the two bands at 1064 and 1130 cm^{-1} to vibrations of skeletal carbon atoms in the trans conformation. The broad envelope of bands centered at 1090 cm^{-1} they assigned to OS vibrations associated with gauche bonds in the chain. Thus when a solid hydrocarbon ($C_{16}H_{34}$) is melted and loses its all-trans character the trans bands at 1064 and 1130 cm^{-1} lose intensity while the 1090 cm^{-1} band increases indicating the formation of rotational isomers. Lippert and Peticolas[9] used this effect to monitor phase transitions in dipalmitoyl lecithin - a model membrane system in which alkyl chains connected to a polar head group are mostly in the trans conformation in the low temperature phase and develop gauche bonds in the higher temperature phase. Similar work on another biomembrane was reported by Lippert and Peticolas,[12] on $C_{16}H_{34}$ by Gaber and Peticolas,[13] and on numbers of hydrocarbons and lipids by Spiker and Levin[14] and by Bulkin and Krishnamachari.[15] In these reports the ratio of trans and gauche band intensities was used as a probe of the relative populations of trans and gauche bonds. Similarly in this paper we have used the intensity ratio I_{1130}/I_{1090} as a qualitative measure of chain straightening or kinking, i.e. a measure of trans/gauche bond population ratios.

Experimental

We have used a gasketed diamond anvil cell[16] (DAC) to obtain high pressure in this experiment, and have followed the ruby fluorescence procedure[17] for measuring pressures in the cell. The DAC has recently been gaining acceptance as a tool for high pressure X-ray spectroscopy and microscopy[18] as well as optical spectroscopy.[19] The simplicity of the device and its relatively low cost make it quite attractive particularly for applications in which the desired pressures are in excess of a few kilobars. The cell is small and easily loaded and manipulated and has a large solid angle for optical experiments. Pressure can be measured fairly quickly by determining the frequency of the peak of the R_1 fluorescence line of a ruby fragment placed in the cell.

There are disadvantages to the DAC however. The diamonds, which serve both as optical windows and as the pressure generating anvils, are birefringent, making polarization studies difficult. We have always used a scrambler before our spectrometer slits to avoid confusion over changing spectral polarization. The diamonds also fluoresce in the presence of the incident laser beam. This fluorescence can be quite troublesome, particularly when the Raman signal is weak, as is the case for the alkanes. The ruby fluorescence can also be a problem, depending upon which laser excitation frequency is used.

To minimize these problems we have taken a number of steps. We have selected diamonds with the lowest possible background fluorescence. Our criterion has been that for excitation with the Krypton laser 752.5 nm light the ratio of the diamond Raman line at 1330 cm^{-1} to the background level

at 1100 cm^{-1} should be greater than 500, and preferably more than 2000. The conventional wisdom is that one should choose type II diamonds for low fluorescence, but we have found some of our best anvils to be gem quality type I stones.

We have generally used one of the krypton laser red lines (647.1, 676.4, and 752.5 nm) for the incident light. The use of red excitation significantly reduces fluorescence. However, since the ruby fluorescence peak occurs at 694 nm, we had to take care in the choice of laser line that the ruby peak would not interfere with the region of the Raman spectrum in which we were interested.

The ruby fluorescence is very strong, but varies as the volume (diameter cubed) of the ruby fragment. Therefore we have tried to use very small ruby samples in our DAC: 50 μm diameter or smaller.

In the lower pressure range of the DAC (up to ~ 70 kbar) one can use larger diamond faces and gasket holes. This has several advantages. The ruby fragment can rest farther away from the region probed by the laser. The laser angle of incidence can be greater which means that the image of the beam as it slants through the diamond before reaching the sample can be partially blocked by the spectrometer slits. This stops some of the diamond fluorescence and flare-induced Rayleigh scattering at the diamond surface from entering the spectrometer. It also allows the specularly reflected laser beam to miss the collection optics. A schematic of the experimental apparatus is shown in Fig. 1. The sample was held in a gasket of thickness 0.3 mm with a hole of diameter 0.3 mm. Pressures ranged up to about 18 kbars. The laser beam power

entering the diamond window was about 120 mW. Most of the data presented here were obtained using the 752.5 nm krypton laser line.

The ruby pressure measurement was made by comparing the fluorescence peak frequency at high pressure with the frequency at room pressure. The fluorescence of the ruby in the pressure cell was excited with the krypton 676.4 nm line. The ruby fluorescence frequency shift was calibrated against a nearby emission peak from an argon lamp. This calibration was used to reduce the effect of a slight nonlinearity and nonrepeatability in the spectrometer wavenumber drive.

Detailed spectroscopic experiments were performed on liquid heptane in the diamond cell. This sample has a strong LAM,and several other acoustic bands in its low frequency Raman spectrum have been identified.[5] Figure 2 shows a pair of heptane spectra, taken at 65°C. The elevated temperature was used so that the sample would remain liquid over a wider range of pressures. In the upper trace of Fig. 2 the sample was held in a capillary at a pressure of one atmosphere. The lower trace was taken at 14.7 kbar in the diamond cell. (The strong new line in the lower spectrum at ~ 1300 cm^{-1} is the diamond Raman line.) Most of the spectral range is only slightly affected by the change in pressure and the band at 1450 cm^{-1} was used as an intensity standard. The frequency range 300 to 600 cm^{-1} contains the acoustic modes, which change quite noticeably with pressure.

In the room pressure spectrum the LAM appears at about 309 cm^{-1}. The band at 507 cm^{-1} results from a molecule with a single gauche bond, TGTT, the band at 363 cm^{-1} is due to the GTTT conformer, and the band at 396 cm^{-1} is caused by a superposition of bands from a single gauche bond molecule, GTTT,

and a double gauche conformer, TTGG.[5] In the high pressure spectrum all the bands have shifted to slightly higher frequencies and a sharp decrease in the LAM intensity is visible.

Figure 3 shows the trend in the intensities of three of the bands mentioned above as a function of pressure. Here the intensities are the integrated intensities under each band profile normalized against the sum of the intensities of the bands. The straight lines in Fig. 3 were obtained by linear least squares fits to the data. We note that when the 1450 cm^{-1} band is used for normalization the intensities of all the acoustic bands drop with increasing pressure, the LAM dropping more quickly than the others.

Similar, though less detailed, experiments were performed on hexane and octane. The results were qualitatively the same: an increase in pressure caused a sharp drop in the relative intensity of the LAM as the other acoustic bands. This can be seen for example in Fig. 4, where low frequency Raman spectra of hexane at room temperature at 1 atmosphere and at 8 kbar are shown. The LAM, at ~ 373 cm^{-1}, is clearly weaker at the higher pressure. As before, the intensities have been normalized to the 1450 cm^{-1} band and, in this case, a broad fluorescence background has been subtracted from the high pressure spectrum.

Since chain stranghtening with pressure was not observed in hexane, heptane or octane, it was decided to examine successively longer chain alkanes. For the longer chains as discussed earlier it is necessary that we shift our attention to the OS region of the spectrum in order to obtain information on conformations. Hexadecane is the shortest alkane whose OS behavior we have

examined as a function of pressure. Figure 5 shows this spectral region from 1000 to 1200 cm^{-1} for hexadecane at a temperature of 136°C at 1 atmosphere in the lower trace and at 8 kbar in the upper trace. These spectra are typical for liquid alkanes. The 1090 cm^{-1} gauche envelope is the strongest feature with the 1060 cm^{-1} trans band a barely visible shoulder on the 1090 cm^{-1} band. The trans band at 1130 cm^{-1} is relatively weak but distinct. The ratio of intensities I_{1130}/I_{1090} is indicative of the trans/gauche bond population ratio, and as can be seen in Fig. 5 there was a slight decrease in this ratio as the pressure rose. In an earlier publication[1] based on preliminary data we stated that we observed no appreciable pressure effect. With better data a slight pressure-induced effect is observable, suggesting a slight kinking of the chain as pressure is incresed.

In sum, then, for a sampling of different short chain alkane liquids, hexane, heptane, octane and hexadecane, we have observed no sign of the chain ordering or chain straightening one might have inferred from the pressure induced effects in polyethylene. Instead we have observed changes in Raman band intensities which indicate pressure induced chain kinking - a dramatic effect in the shorter chains, a slight effect for hexadecane. In the following section we offer a theoretical model as a possible explanation of this short chain effect.

Theory and Comparison with Experiment

The conformational structure of an n-alkane can be specified in terms of n-3 dihedral angles corresponding to the n-3 internal C-C bonds. For the liquid and gas states the intramolecular interactions are the most important factor in determining the equilibrium statistical distribution of these angles. Scott and Scheraga[20] have introduced a semiemperical model for this intramolecular potential energy. As a function of the dihedral angle Q, there are three minima in this function corresponding to trans (Q = 0), right gauche (Q = 120°) and left gauche (Q = -120°). The model potential energy is large compared with typical values of $K_B T$, except for Q in the neighborhood of one of the three minima. For this reason it is customary to characterize an internal C-C bond as being in either the trans or gauche state, and to specify the conformational state of a molecule by the number and sequence of trans and gauche bonds.

According to the Scott-Scheraga model potential, the gauche state energy is about 700 cal/mole higher than the trans state. This energy difference is the sole factor in determining the trans/gauche population ratio in the gas state. Studies of trans/gauche population ratios in liquids however, have traditionally been interpreted as implying that the trans-gauche energy difference is 500 cal/mole for the condensed state.[21]

Evidentally the liquid environment causes some lessening of the favoratism for the trans conformations. However, it is naive to think that this is simply a dielectric effect because in the condensed state, hard core repulsive interactions are more important in determining structure than attractive

interactions. A brief examination of the problem of an n-alkane dissolved in a hard sphere solvent shows the importance of the hard core interactions. For instance, in the case of butane dissolved in CCl_4, the somewhat compact gauche conformation is more favored by the solvent effect than is the linear fully extended trans conformation - a result derived by a consideration of cavity correlation functions in a hard sphere liquid.[22]

The calculations in Ref. 22 are necessarily complicated because they use an approach which is capable of producing a good equation of state for the hard sphere liquid. However, a rough argument from the vantage point of Ref.22 shows that the trans population should be reduced in the liquid state. The (mixed) second virial coefficient for a hard sphere of diameter b and a hard spherocylinder of diameter a and length ℓ+ a is one-half the volume excluded to the center of the sphere by the presence of the spherocylinder. (A spherocylinder is a cylinder of length ℓ capped by hemispheres of diameter a at both ends.) This viral coefficient is easily calculated to be

$$B_{sc} = \frac{\pi}{12} (a + b)^3 + \frac{\pi}{8} (a + b)^2 \ell \qquad (1)$$

On the other hand the virial coefficient for a sphere of diameter b and a sphere of the same volume as that of the spherocylinder above is

$$B_{ss} = \frac{\pi}{12} (a(1 + \frac{3\ell}{2a})^{1/3} + b)^3 \qquad (2)$$

For $\ell > 0$ and $b > 0$, $B_{sc} > B_{ss}$. Therefore, spheres can be packed into a liquid of spheres with less "wasted space" than spherocylinders of the same volume as the spheres. Consequently it is to be expected that molecular

conformations that are more nearly spherical than the linear all trans conformation are favored over the all trans conformation in quasi spherical solvents. The same considerations also apply to a neat butane liquid as was demonstrated in Ref. 22. Thus, hard sphere interactions with entropy correctly taken into account appear to be relevant to the problem of calculating conformational populations in condensed systems. Below, we will apply a hard rod packing approach to the problem of pressure effects on conformational populatiosn in n-alkane fluids.

The rough virial coefficient argument given above and the work of Ref. 22 indicate that globular conformations are increasingly favored as the pressure is increased. It is of value therefore, to present a self-contained model calculation producing this result. Self-consistent calculations of the number of ways of packing N rods into a volume V have been pursued for many years in the field of liquid crystals.[23-25] The structure of these liquid crystal calculations has some of the elements of the virial coefficient argument above. These calculations rely on the mean field approximation and hence are not on as firm a foundation as those based on hard sphere correlation functions. However they have the advantage that they are not restricted to nearly spherical molecules.

The evaluation of the number of ways of packing hard rods into a fixed volume is equivalent to a calculation of the translational entropy of the hard rod fluid. Traditionally, these calculations have been used to study the onset of long range orientational order. The use of the mean field approximation causes neglect of short range order and correlations. The chief result of this neglect seems to be that the liquid crystal calculations give poor results for the equation of state while long range orientational order is predicted reasonably well. Thus, based on the results of the liquid crystal calculations

we expect the results to be reasonable except where quantities pertaining to the equation of state are encountered.

In the absence of long range orientational order the packing calculation in the mean field approximation reduces to calculating the number of ways of packing N totally uncorrelated hard rods of aspect ratio X into a volume V. The results of the calculations can be summarized in an equation [25] for the translational entropy S in units of Boltzmann's constant:

$$S/K_B = f(\rho) - g(\rho)\, B(X) \tag{3}$$

Here ρ is the ratio of density to a close packing density. The small ρ of expansions of f and g are related to virial series. Both f and g diverge as ρ approaches unity. We have $g > 0$, $dg/d\rho > 0$, $B > 0$ and $dB/dX > 0$. The exact form of the functions f,g and B vary according to the method of calculation. The quantities $f(\rho)$ and $g(\rho)$ are intimately related to the equation of state in these theories and their detailed forms cannot be specified accurately. If we allow there to be M species of molecules corresponding to M distinct conformations, the free energy per molecule becomes:

$$F/K_BT = -f(\rho) + \sum_{i=1}^{M} [h_i W_i \ell n(h_i) + \varepsilon_i h_i W_i / K_B T + g(\rho)\, h_i W_i B(X_i)] \tag{4}$$

Here h_i is the fractional population of the ith species ($\Sigma h_i = 1$), T is the temperature, W_i is the combinitorial weight of the i^{th} distinct species, (conformations differing only in chirality are not considered distinct) and ε_i is the Scott-Scheraga energy associated with the i^{th} conformation. The energy ε_i is proportional to the number of gauche bonds in the i^{th} conformation. The

population on the ith species is found by minimizing F with respect to the h_i

$$h_i = h_i'/\Sigma_i h_i' W_i \tag{5}$$

$$h_i' = \exp[-\epsilon_i K_B T - B(X_i)g(\rho)] \tag{6}$$

Since the all-trans conformation has the largest value of X it is clear that the population of the all-trans conformation will decrease as ρ increases and hence as the pressure increases.

In order to obtain more specific predictions from equation 6 we require detailed knowledge of ϵ_i, $B(X_i)$ and $g(\rho)$. As mentioned above, the mean field approximation liquid crystal theories can not be expected to give accurate results for $g(\rho)$. To calculate $B(X_i)$ we take Alben's form for spherocylinders

$$B(X) = (\frac{7}{6} a^3 + \frac{7}{4} a^2 \ell + \frac{1}{2} a\ell^2)/(a^3/6 + a^2\ell/4) \tag{7}$$

with $\ell/a = X-1$, and use space filling molecular models to estimate ℓ/a. For heptane the range of B(X) is from 9.3 for the all trans conformation to 8.0 for the four gauche conformation. A problem with the use of these figures is that the theory has neglected short range orientational correlations. Consequently the ordering of the values of B(X) is correct but the range of B(X) may be over (or under) estimated. This will not be a problem for the calculation below because it can be compensated for by appropriately scaling the unknown function $g(\rho)$ by a constant factor. However this scale factor will be different for longer molecules. This makes it difficult to draw quantitative conclusions about the behavior of longer molecules subjected

to high pressure. In the extreme case the theory breaks down. It is known that polyethylene does not tend to become globular at high pressure. This is not a contradiction because orientational correlations, here neglected, are expected to become increasingly important as the molecular aspect ratio increases.

The problem of the lack of knowledge of the form of $g(\rho)$ and of the scaling factor mentioned above can be sidestepped by eliminating $g(\rho)$ in equation (6) in favor of h_1, the population of the all trans conformation if the set of ϵ_i are known. Of course $\epsilon_i = n_i E_o$ where n_i is the number of gauche bonds in the i^{th} conformation and E_o is the trans-gauche energy difference for a single bond. (We take the value of ϵ_i for <u>sterically</u> forbidden conformations to be infinite). The traditionally accepted value of E_o in condensed systems is 500 cal/mole. If we use this value we must set $g(\rho_o) << 1$ where ρ_o corresponds to atmospheric pressure. On the other hand the gas phase value of E_o is 700 cal/mole. If we use this value and choose the scaled value of $g(\rho_o)$ equal to .8, we get approximately the same conformational populations as above. The temperature dependence of the populations at constant density is of course, different for these two choices of E_o. However, it must be kept in mind that at constant pressure ρ_o is a function of temperature by virtue of thermal expansion. This implies that $g(\rho_o)$ is a decreasing function of temperature. This means that the packing term favoring gauche conformations becomes less effective as the temperature increases. This will cancel out some of the effect of $E_o = 700$ cal/mole. The behavior could very well mimic $E_o = 500$ cal/mole and $g(\rho_o) << 1$ over a restricted

temperature range. This issue is discussed in more detail in Ref. 22.

In principle the high pressure experiments done at different temperatures can lead to a determination of the correct value of E_o for condensed systems. As a practical matter two factors make this aim difficult to achieve, First, as noted above, the correct scaled form of $g(\rho)$ is unknown. Second, the Raman intensities can not be expected to be in a strictly linear relationship with the conformational populations. Any non linearity would affect the value of E_o deduced.

In Fig. 6 we have plotted the conformational populations of hexane as functions of P_o/P_o^*, the population of the all trans conformation. The open circles are experimental points obtained from the Raman experiment. The smooth curves were calculated from equation 6 using E_o = 500 cal/mole. The lower curve is the sum of the populations in the two distinct single gauche conformations. The upper curve is the calculated population of the conformations having two or more gauche bonds. These include 6 conformations with 2 gauche bonds, 3 with 3 gauche bonds and one with 4 gauche bonds. The populations of the 12 conformations which are sterically forbidden are zero. The abscissa, the population in the trans conformation, has been normalized to unity at the point corresponding to $g(\rho) = 0$. This is regarded as corresponding to atmospheric pressure. The value of $g(\rho)$ associated with each value of the absiccsa increases to the left implying that pressure increases to the left. A very similar set of curves would be generated if E_o were chosen as 700 cal/mole. However, as discussed above, quite different values of $g(\rho)$ would be associated with each value of the abscissa.

The agreement with the experimental points is quite good considering the approximations made in the theory. It is particularly significant that the populations of the single gauche conformations decrease along with that of the all trans conformation as the pressure increases.

Conclusion

Raman scattering intensities of conformationally sensitive optic vibrations in linear alkanes have shown that pressures of several kilobars cause some chain molecules to become kinked. This effect has been observed in chains as long as $C_{16}H_{34}$. The conformational changes are indicated by changes observed in the acoustic modes and the optical skeletal modes. A theory based on considerations of conformational energy and translational entropy has been developed which suggests that the observed kinking is to be expected for the shorter chain linear alkanes. Since there may be an ordered phase in polyethylene liquid at high pressure and since such an ordered phase does not appear to exist for shorter chain alkanes, one might expect there to be a "crossover" chain length above which such a phase could be observed. A search for such a "crossover" chain length is continuing with longer alkanes and polyethylenes of varying molecular weight.

Acknowledgement: We gratefully acknowledge the partial support of the Office of Naval Research for some of the work reported herein.

References

1. P. E. Schoen, R. G. Priest, J. P. Sheridan and J. M. Schnur, Nature, 270, 412 (1977).

2. L. S. Bartell and D. A. Kohl, J. Chem. Phys. 39, 3097 (1963).

3. K. Monobe, Y. Fujiwara and I. Tanaka, Proceedings of the 4th Intl. Conf. on High Pressure, Kyoto, 1974 (Kawakita, Kyoto, 1975) p.63 and 865.

4. S. -I. Mizushima and T. Shimanouchi, J. Am. Chem. Soc. 71, 1320 (1949).

5. R. F. Schaufele, J. Chem. Phys. 49, 4168 (1968).

6. R. G. Snyder, J. Chem. Phys. 47, 1316 (1967).

7. R. F. Schaufele and T. Shimanouchi, J. Chem. Phys. 47, 3605 (1967).

8. R. G. Snyder, J. R. Scherer, J. Mazur and B. Fanconi, Bull. Am. Phys. Soc. 23, 404 (1978).

9. J. L. Lippert and W. L. Peticolas, Proc. Nat. Acad. Sci. 68, 1572 (1971).

10. M. Tasumi, T. Shimanouchi, and T. Miyazawa, J. Mol. Spectrosc. 9, 261 (1962).

11. R. G. Snyder and J. H. Schachtschneider, Spectrochim. Acta. 19, 85 (1963).

12. J. L. Lippert and W. L. Peticolas, Biochim. Biophys. Acta. 282, 8 (1972).

13. B. P. Gaber and W. L. Peticolas, Biochim Biophys. Acta. 465, 260 (1977).

14. R. C. Spiker and I. W. Levin, Biochim. Biophys. Acta. 388, 361 (1975); and 433, 457 (1976).

15. B. J. Bulkin and N. Krishnamachari, J. Am. Chem. Soc. 94, 1109 (1971).

16. P. E. Schoen, J. M. Schnur, and J. P. Sheridan, Appl. Spectros. 31, 337 (1977).

17. J. D. Barnett, S. Block, and G. J. Piermarini, Rev. Sci, Instrum. 44, 1 (1973).

18. D. C. Bassett, S. Block, and G. J. Piermarini, J. Appl. Phys. 45, 4146 (1974).

19. B. A. Weinstein and G. J. Piermarini, Phys. Lett. 48A, 14 (1974); and D. M. Adams, S. J. Payne, and K. Martin, Appl. Spect. 27, 377 (1973).

20. R. A. Scott and H. A. Scheraga, J. Chem. Phys. 44, 3054 (1966).

21. P. J. Flory, Statistical Mechanics of Chain Molecules, (Interscience, New York, 1969).

22. L. R. Pratt and D. Chandler, J. Chem. Phys. 68, 4202 (1978); and C. S. Hsu, L. R. Pratt and D. Chandler, J. Chem. Phys. 68, 4213 (1978).

23. R. Alben, Mol. Cryst. Liq. Cryst. 13, 193 (1971).

24. G. Lasher, J. Chem. Phys. 53, 4141 (1970).

25. R. G. Priest, Phys. Rev. 8, 3191 (1973).

Figure Captions

Figure 1 - Schematic of setup: Light from a Kr^+ laser is focused by a small, off-axis mirror into the diamond cell (inset shows expanded view of the gasket sandwiched between the diamond anvils). Scattered light is collected and focused into the Spex Raman monochromator through a polarization scrambler (S).

Figure 2 - Raman spectra of heptane at 65°C. Upper trace: one atmosphere. Lower trace: 14.7 kbar. Large feature running off scale in lower trace at about 1300 cm^{-1} is the diamond Raman line.

Figure 3 - Integrated intensities of three acoustic bands of heptane vs. pressure at 65°C. Intensities are normalized to the sum of the three band intensities. The 504 and 405 cm^{-1} bands are due to gauche rotational isomers and the 312 cm^{-1} band to the all-trans conformer.

Figure 4 - Raman spectra of hexane in the acoustic region at room temperature. LAM is sharp feature at ~ 373 cm^{-1}. Trace A: 1 atmosphere; trace B: 8 kbar.

Figure 5 - Raman spectra of hexadecane in the optical skeletal region at 136°C. Gauche envelope is large feature at ~ 1090 cm^{-1}. A very weak trans bond appears as a shoulder at ~ 1060 cm^{-1} and another trans band occurs at ~ 1130 cm^{-1}. Upper trace: 8 kbar; lower trace: 1 atmosphere.

Figure 6 - Relative gauche conformer populations from the acoustic band intensities. Lower curve: relative population, P_1, of molecules with one gauche bond. Open circules are data points. Lines are theoretical curves. Upper curve: sum of populations of conformers with 2, 3, and 4 gauche bonds, P_{2-4}. The abcissa is the all-trans population, P_o, relative to its room pressure value, P_o^*. Pressure is increasing to the left.

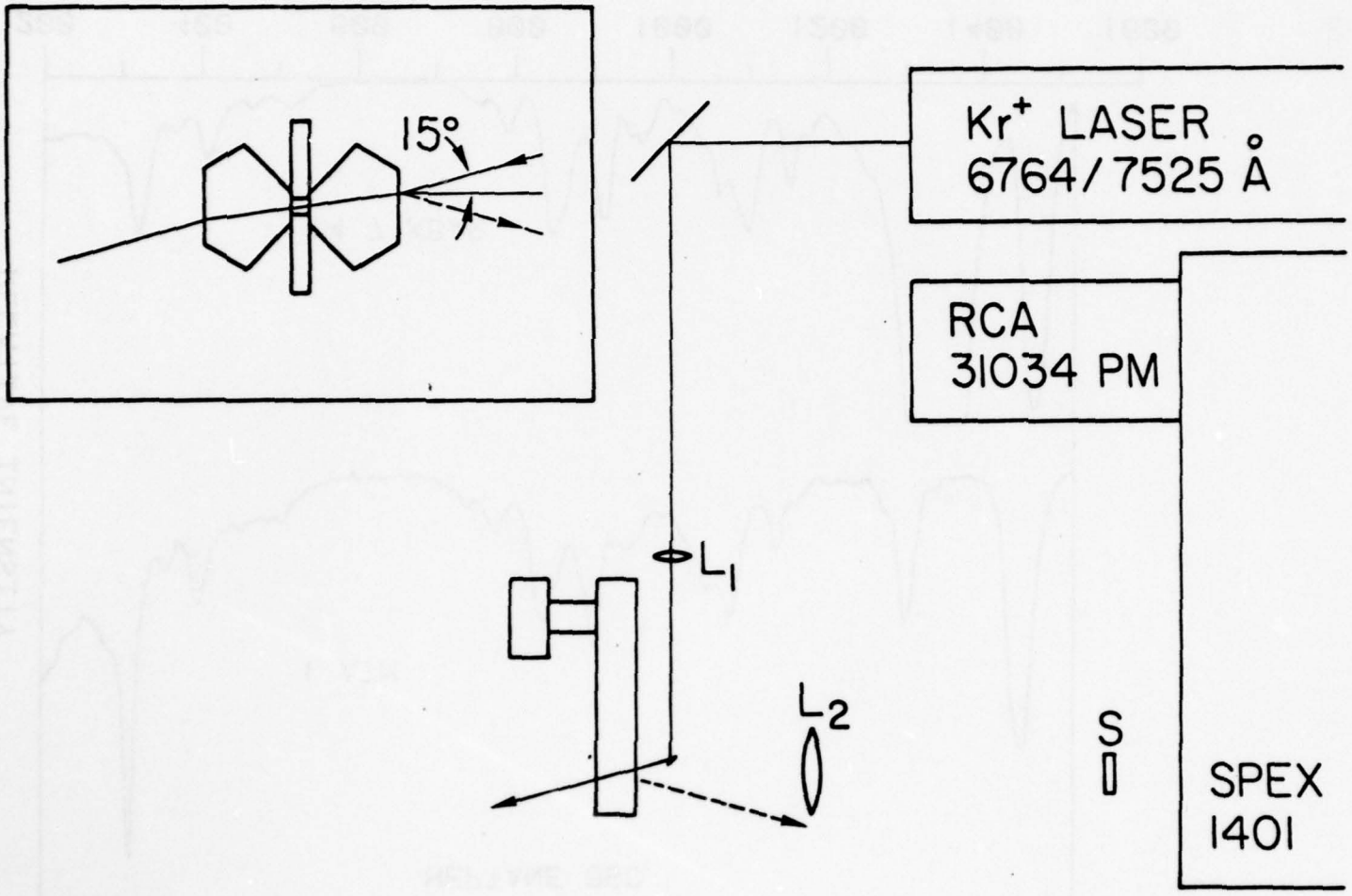

Figure 1

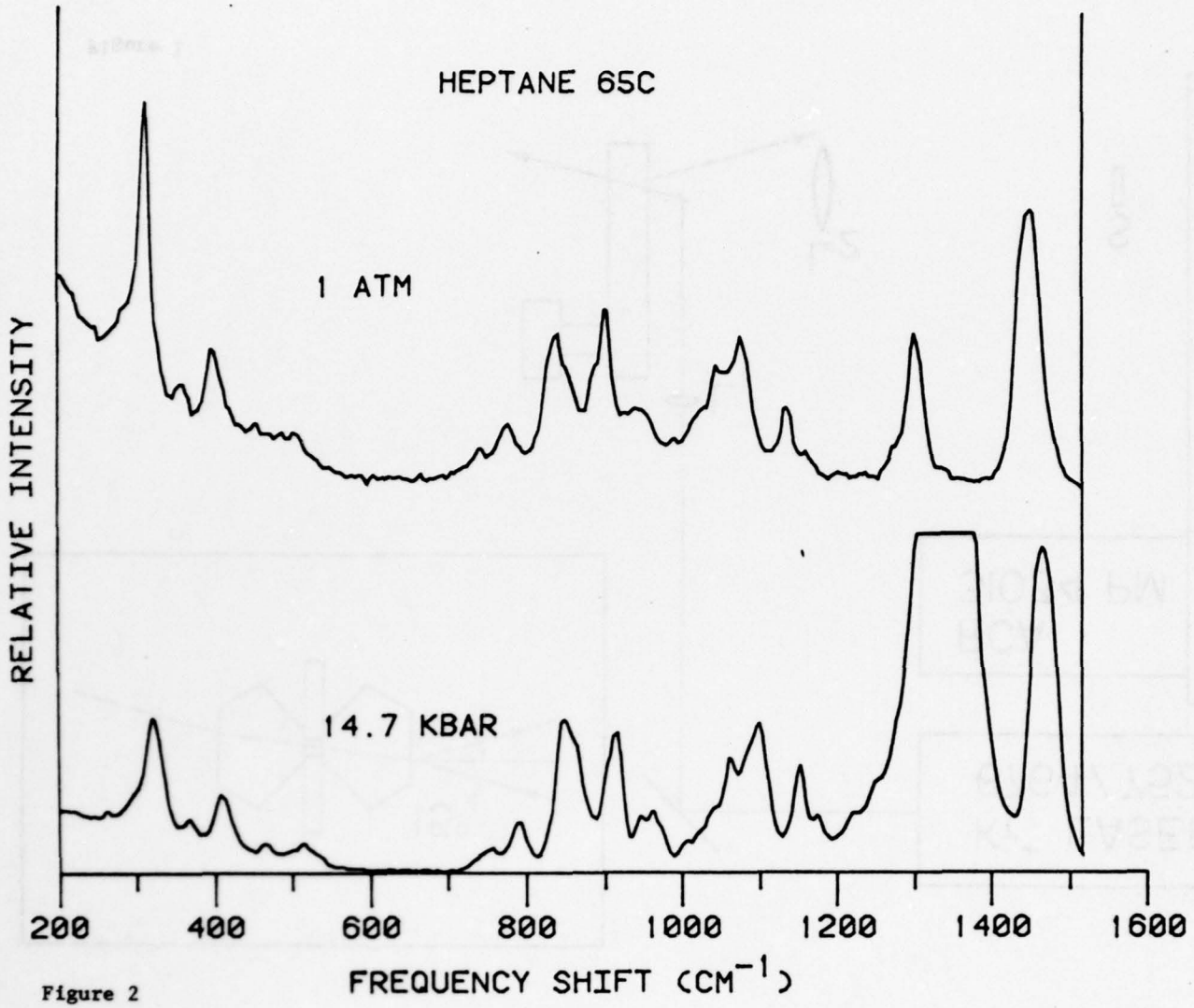
HEPTANE 65C
1 ATM
14.7 KBAR
RELATIVE INTENSITY
200
400
600
800
1000
1200
1400
1600
FREQUENCY SHIFT (CM^{-1})

Figure 2

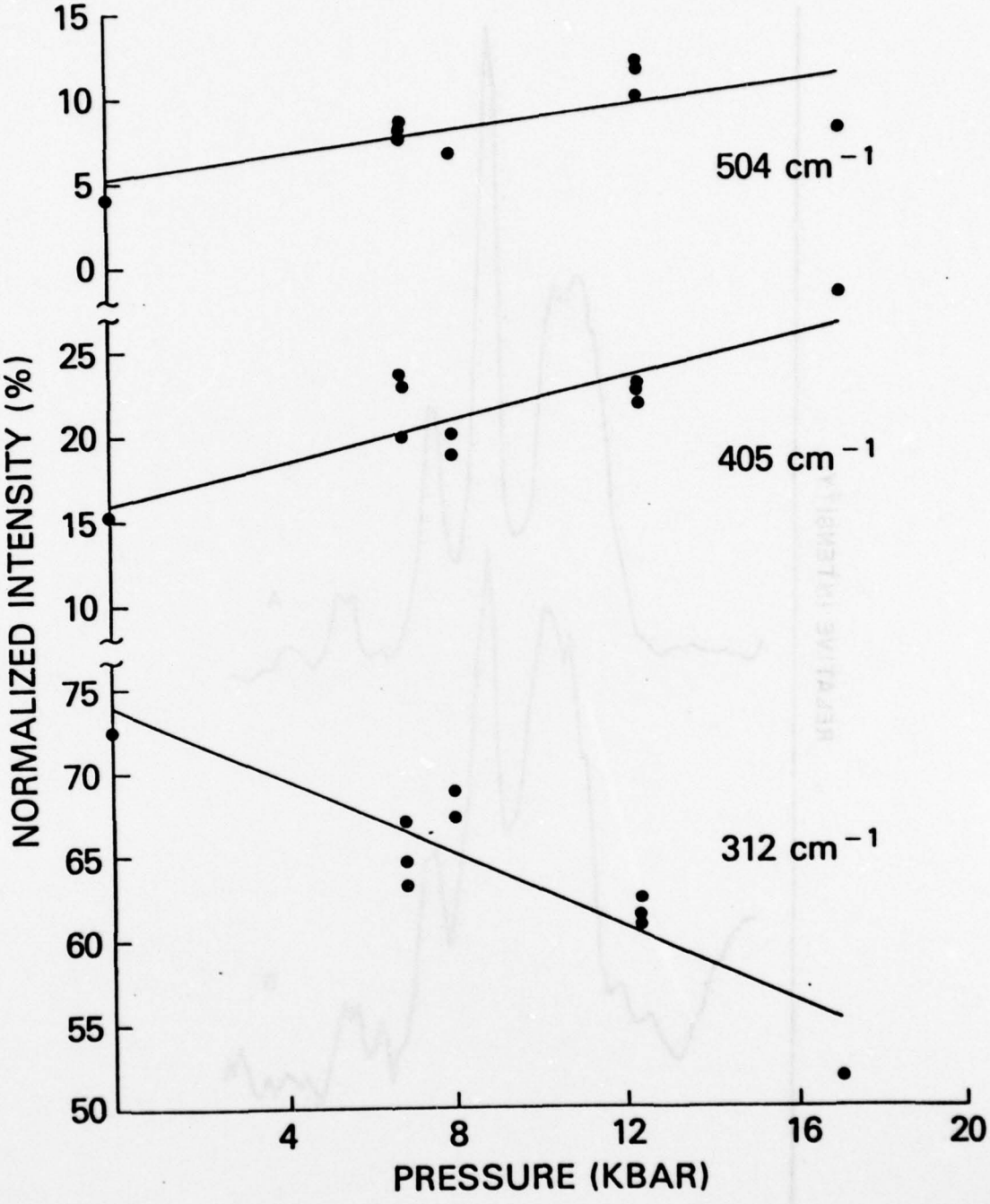
NORMALIZED INTENSITY (%)
15
10
5
0
25
20
15
10
75
70
65
60
55
50
504 cm⁻¹
405 cm⁻¹
312 cm⁻¹
4
8
12
16
20
PRESSURE (KBAR)

Figure 3

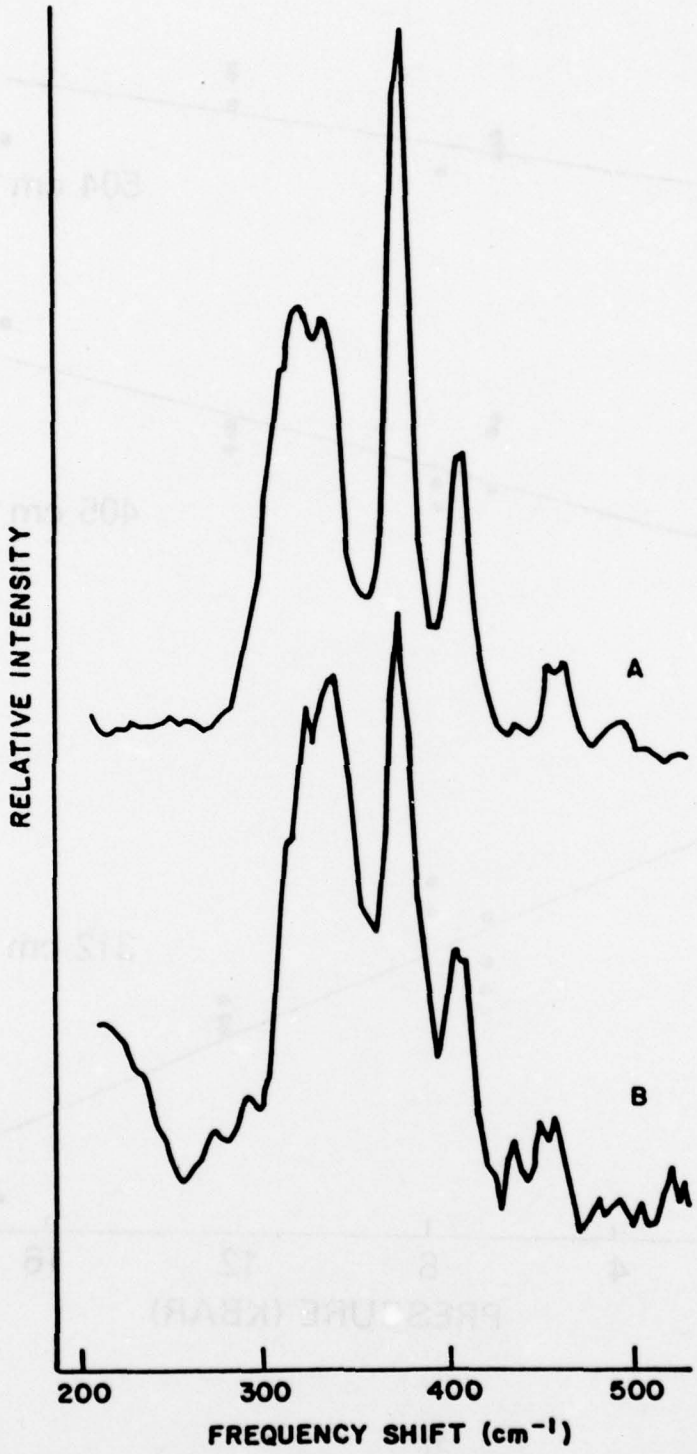

Figure 4

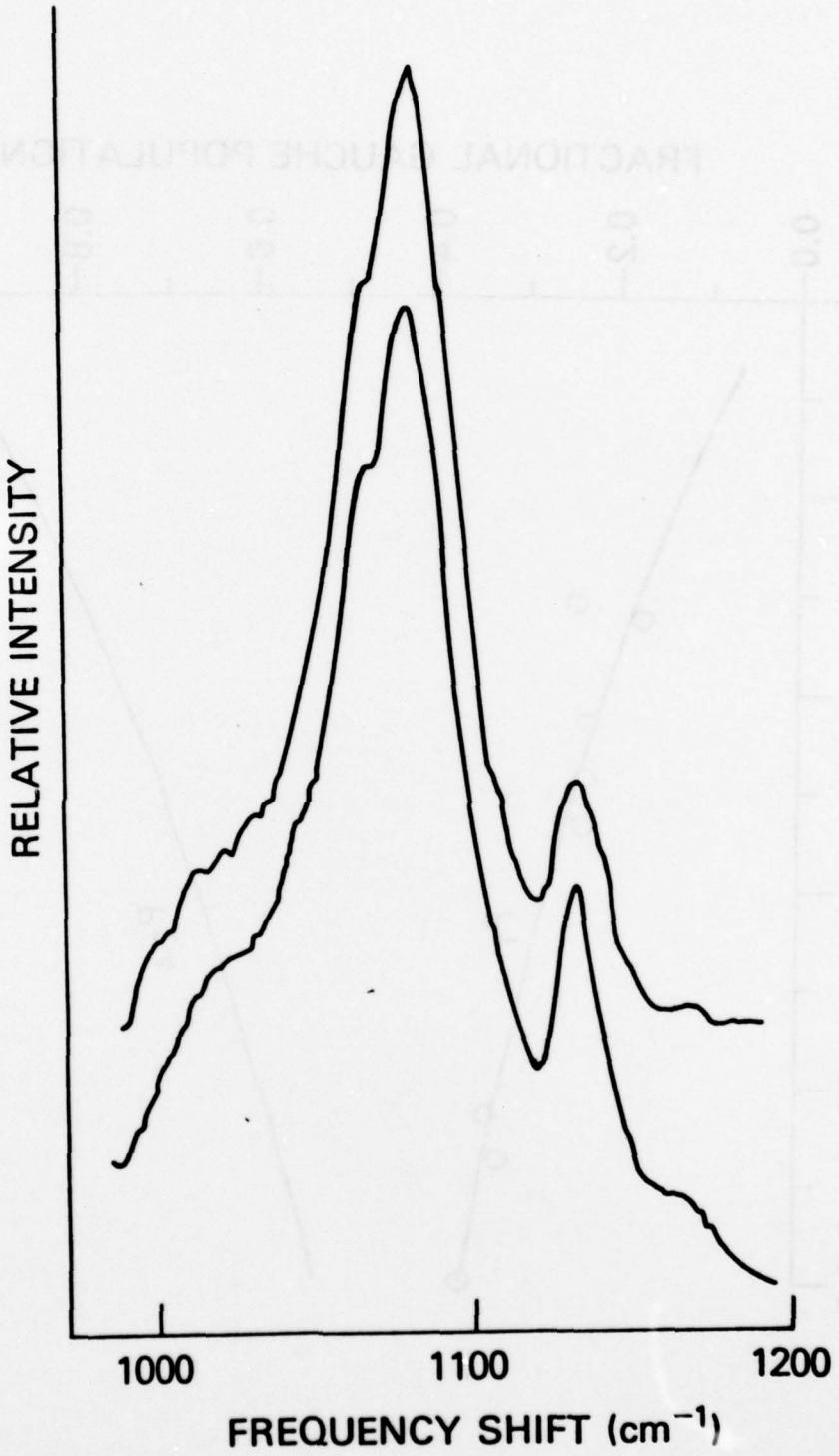

Figure 5

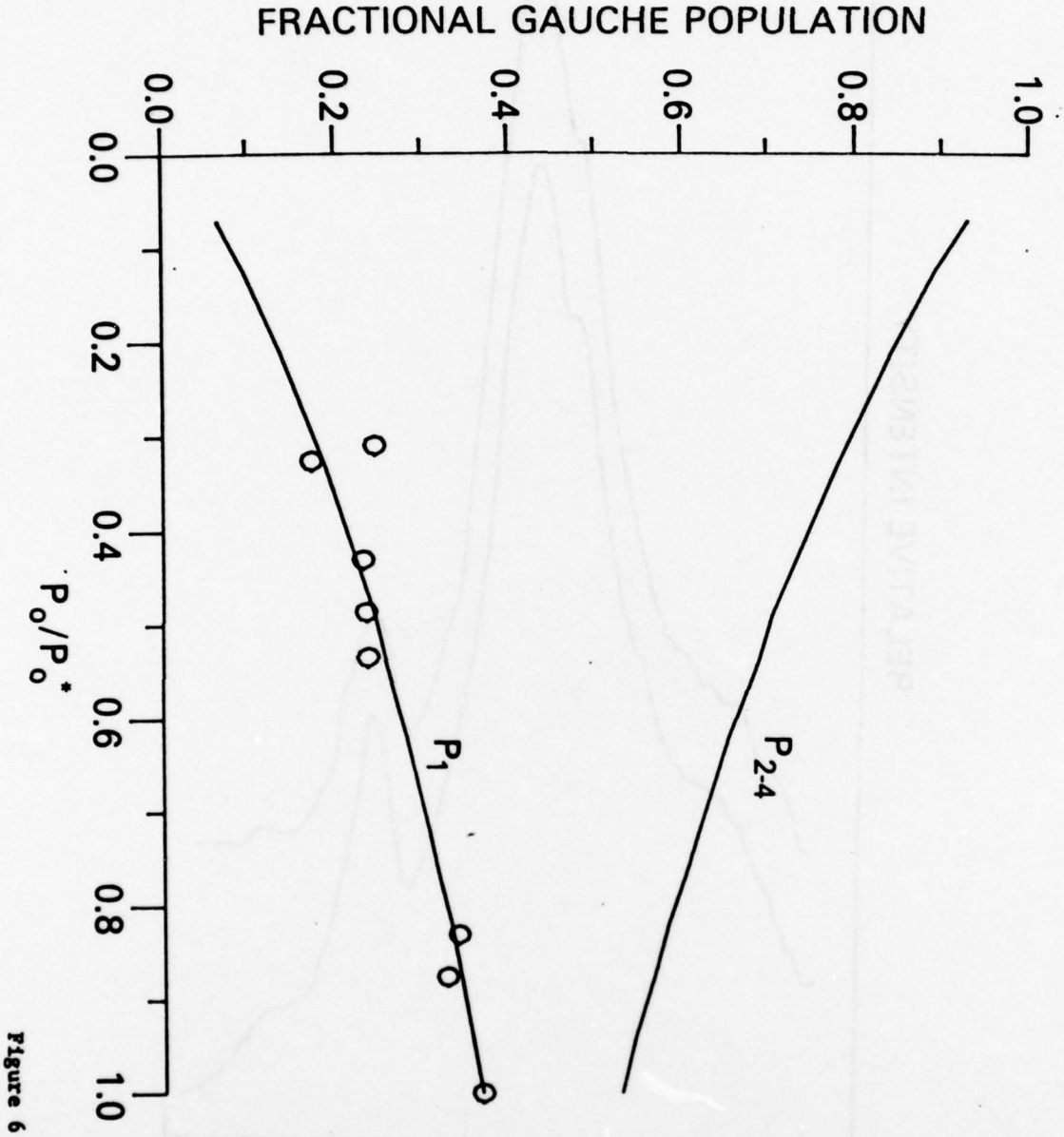

Figure 6

RAMAN SCATTERING FROM POLYETHYLENE AND THE HIGH MOLECULAR WEIGHT ALKANES UNDER PRESSURE

by
S. L. Wunder, F. Cavatorta, R. G. Priest, P. E. Schoen, J. P. Sheridan
J. M. Schnur
Naval Research Laboratory
Washington, D. C. 20375

Introduction

Efforts to enhance polymer mechanical properties by alteration of the crystalline structure from one with lamellar morphology to one with an extended chain conformation have been of ongoing interest in polymer research. The observation by Japanese workers[1,2] using DTA that an ordered liquid phase exists in polyethylene at elevated pressures before crystallization to the extended chain morphology suggests that pressure can be used as a variable to obtain molecular ordering in polymers. Previous work in this laboratory on the low molecular weight alkanes[2] (C_7 and C_{16}) showed in contrast that these molecules "kinked-up" under pressure. Therefore, it is to be expected that a crossover chain length exists in which pressure causes chain straightening. In the present work the behavior of alkanes in the mid molecular weight range was studied spectroscopically. C_{40} and C_{44} were chosen because their crystalline morphology, the orthorhombic sublattice, is isomorphic to that of polyethylene. It was found that both C_{40} and C_{44} exhibited a marked increase in the ratio of trans to gauche bonds with increasing pressure in the melt.

Experimental

Raman scattering from a diamond anvil cell (DAC) was used as a molecular probe to follow conformational changes in the alkanes under pressure. The pressure measurements were obtained from the pressure dependent frequency shifts of the ruby R_1 and R_2 lines. The Raman spectra of the alkanes is weak compared to both diamond and ruby fluorescence, so procedures had to be adopted to maximize the alkane signal. This was achieved by increasing the sample volume, decreasing the size of the ruby chip used and choosing diamonds with intrinsically low fluorescence. The gasket holding the sample was 0.78 mm thick with a hole drilled in it of diameter 0.64 mm. The diamond faces were 0.8 mm each. The alkane spectra were obtained using the 6764 Å line of a Model 52 Krypton ion laser while the 6471 Å line was used for the pressure measurements.

Since C_{40}, C_{44} and polyethylene, unlike the lower molecular weight alkanes, are solid at room temperature and pressure (RT&P), they had to be melted under pressure in the DAC. Experiments were performed by varying pressure at constant temperature. The latter was maintained constant using a dual heating system and was measured using ultra-thin copper-constantan thermocouple wire attached directly to the gasket. Temperature control was thus achieved to within ± 0.2°C. Pressure measurements were accurate to within $\pm$ 1.5 kbar, but refinements in the ruby fluorescence technique as applied to this system have subsequently lead to substantial reduction in this uncertainty.

The alkane samples C_{40} and C_{44} were used as received from Pressure Chemicals. Analysis on a gas chromatograph indicated that their purity was at least 99%.

Results and Discussion

Figure 1, the Raman spectra of C_{40} in the melt at 150°C as a function of increasing pressure, is representative of the spectral changes which

occur and which reflect the changing molecular conformations and environmental conditions of the molecules. Four regions of the Raman spectra were observed. The longitudinal acoustic mode (LAM) is due to a vibration of the molecule in the all trans configuration; it is a totally symmetric accordion-like motion which occurs in the low frequency regime. The optical skeletal modes occur between 1000 cm^{-1} and 1200 cm^{-1}; the bands at 1060 cm^{-1} and 1140 cm^{-1} are attributed to symmetric and antisymmetric C-C-C stretches involving trans bonds; the envelope of bands centered around 1080 cm^{-1} which occurs in the melt spectra is due to vibrations involving gauche bonds. Raman shifts in the region 1400 cm^{-1} to 1500 cm^{-1} are attributed to H-C-H bending vibrations. The H-C-H stretching vibrations occur in the high frequency region between 2800 cm^{-1} and 3000 cm^{-1}; the bands at 2850 cm^{-1} and 2887 cm^{-1} have been assigned to symmetric and antisymmetric stretches, respectively. The H-C-H modes are sensitive to environmental conditions.

In the solid at RT&P, as seen in Figure 2, virtually no bands associated with gauche bonds exist. In the melt spectra of Figure 1, initially most of the C-C stretch intensity is associated with gauche conformers, but signal from trans sequences also exists and increases with pressure until the all trans configuration occurs with great enough statistical weight to result in the appearance of a LAM. The LAM appears at around 70 cm^{-1} at 5-6 kbar; at RT&P it occurs at 61.5 cm^{-1}. Since no internal standard exists with which to normalize LAM intensities, comparison as a function of pressure was not possible. Spectra in the LAM region are not shown due to lack of space.

The trans/gauche ratio was determined from the ratio of peak heights of the 1140 cm^{-1} to 1080 cm^{-1} bands. Since these ratios are not linearly related, their functional dependence was determined empirically in an independent set of experiments. The statistical weights of the conformers were calculated in the rotational isomeric state approximation assuming a Boltzmann distribution; the only short range intramolecular correlation considered was that due to pentane exclusion. The calculated populations were correlated with intensity ratios from C_{40} samples measured at room pressure, where the temperature was varied to change the relative populations. This data was then used to obtain a calibration curve. Comparison of the experimental trans/gauche ratios obtained as a function of pressure with this curve indicate that the population of trans bonds increases from about 60% to over 95%. At pressures at which the LAM appears, the gauche population is still around 20-30%.

The bands between 1400 cm^{-1} and 1500 cm^{-1} are affected by Fermi resonance effects, so their interpretation is more complicated. According to Snyder,[4] the orthorhombic crystal at RT&P has a fundamental at 1142 cm^{-1} which is split by the crystal field into components at 1418 cm^{-1} and 1449 cm^{-1}. The latter has a Fermi resonance interaction with overtones of the 720 cm^{-1} rocking fudnamental giving rise to bands at 1440 cm^{-1} and 1462 cm^{-1}. These three bands can be observed in the solid spectrum (Figure 2). The melt spectrum at RT&P (not shown) looks identical to Figure 1a; there is one slightly asymmetric band centered around 1440. With increasing pressure, a band around 1420 appears, which eventually becomes larger than the 1440 cm^{-1} band. All that can be presently said about this band is that it is consistent with either an hexagonal lattice correlation split by Fermi resonance (the hexagonal lattice has only one molecule per unit cell and therefore cannot be crystal field split) or with an ordered liquid phase exhibiting Fermi resonance. An hexagonal lattice is the crystal form assumed by the "rotator phase." This is believed to be a solid phase occurring in the n-alkanes a few degrees below their melting points and has been associated with the onset of

hindered rotation of the extended chains about their long axes. Barnes and Fanconi[5] found that the spectrum of this phase was much closer to that of the crystal than to that of the melt and was inconsistent with a "kink-back" model hypothesized for the "rotator" phase which would require about 30% gauche bonds. A rotator phase was ruled out here since DTA measurements[6] indicate that the "rotator phase" does not exist in alkanes above C_{44} and, more importantly, is squeezed out as a function of pressure.[7] The high frequency spectra shown in Figures 1 and 2 are also complicated by Fermi resonance. An attempt to explain these effects will not be made. It is noted however, that the solid spectra is typical of that of an orthorhomic crystal. The melt spectra of Figure 1a is the same as that of the melt spectra at RT&P. With increasing pressure the appearance changes to that expected of an hexagonal lattice, but as noted by Snyder,[4] the high frequency spectrum of the latter and the melt closely resembly one another.

Conclusions

The effect of pressure on the melt phase of the mid molecular weight alkanes is to cause an increase in ordering of the chains as observed by the marked increases in trans to gauche ratios. It was not possible using spectroscopic techniques alone to determine whether this occurs gradually or abruptly as the result of a phase transition. Data on polyethylene where preliminary calorimetric work to map out the phase diagram has already been performed[2] will be reported. The power of high pressure Raman spectroscopy to help elucidate the molecular changes which occur as polyethylene forms the extended chain conformation has been demonstrated.

References

1. M. Yasuniwa, C. Nakafuko and T. Takemura, Polymer J. 4, 526 (1973).

2. K. Monobe, Y. Fujiwara and K. Tanaka, Proc. Int. Conf. High Pressure, 4, 63 (1974).

3. P. E. Schoen, R. G. Priest, J. P. Sheridan, J. M. Schnur, Nature 270, 412 (1977).

4. R. G. Snyder, S. L. Hsu and S. Krimm, Spectrochem. Acta 34, 395 (1978).

5. J. D. Barnes and B. M. Fanconi, J. Chem. Phys. 56, 5190 (1972).

6. M. G. Broadhurst, J. Res. Nat. Bur. Stand. Sect. A66, 241 (1962).

7. A.Wurflinger and G. M. Schneider, Ber. Bunsenges, Phys. Chem. 77, 121 (1973).

Figure 1
Raman spectra of melted C_{40} at T=150°C under increasing pressure. Pressure is about 5 kbar with spectral changes occuring over a 1.5 kbar interval. Intensities are all unnormalized.

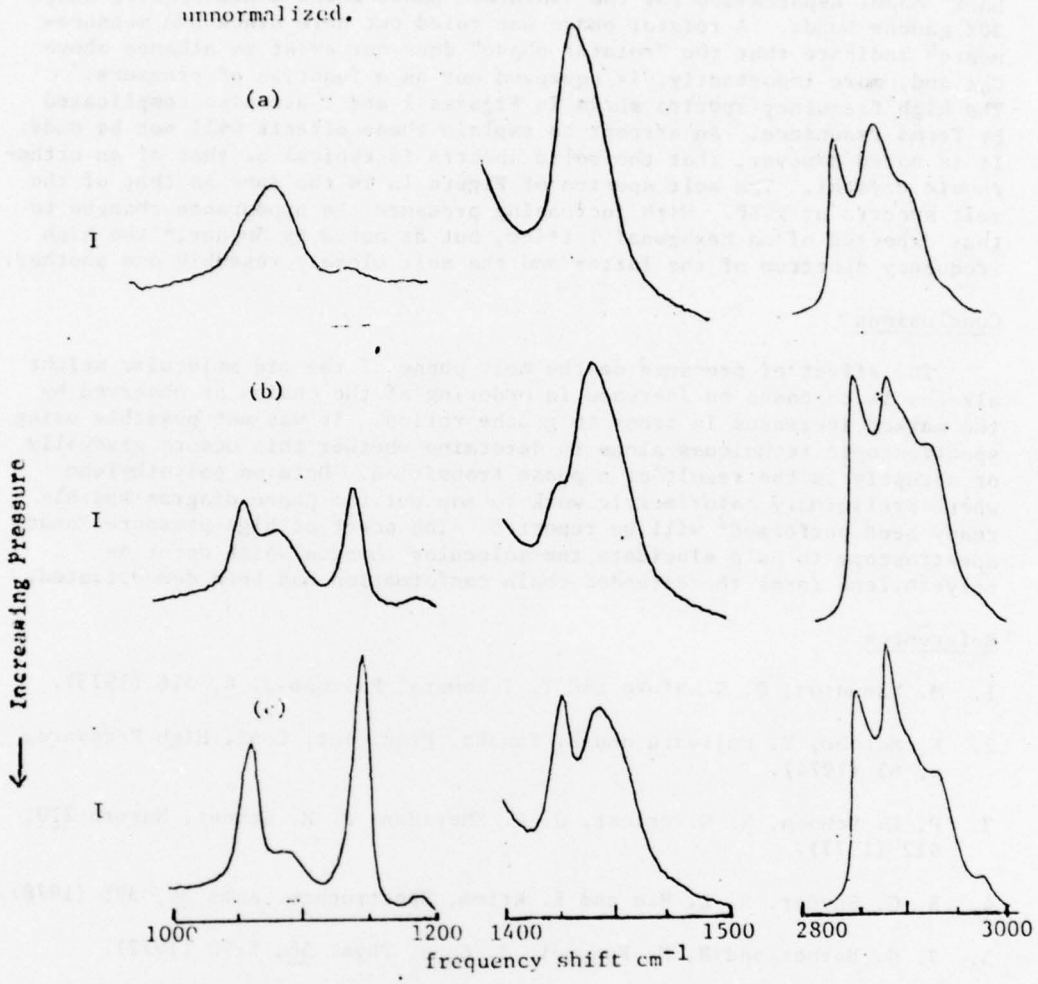

Figure 2
Raman spectra of solid C_{40} at T=25°C and P=1 atmosphere. Intensities are unnormalized.

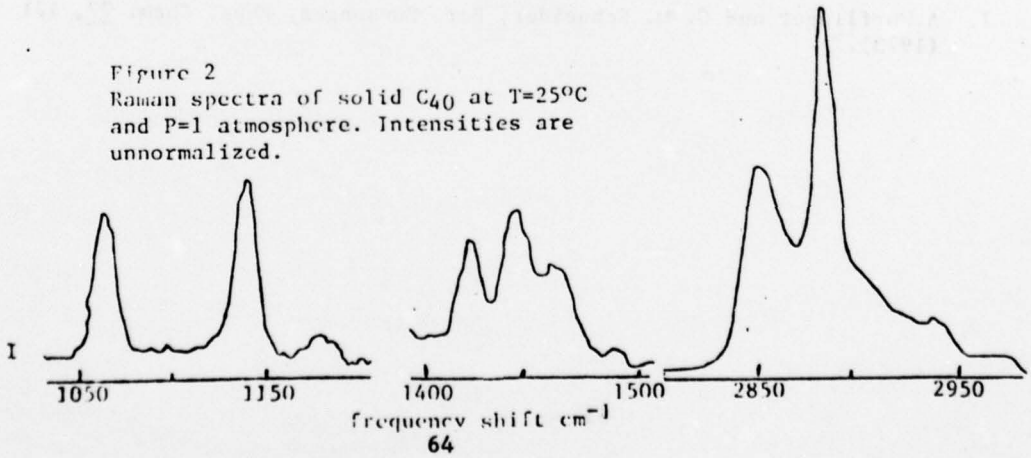

Picosecond Phenomena

Proceedings of the First International Conference
on Picosecond Phenomena
Hilton Head, South Carolina, USA
May 24–26, 1978

Editors
C. V. Shank E. P. Ippen S. L. Shapiro

With 222 Figures

Springer-Verlag Berlin Heidelberg New York 1978

SHORT PULSE ABSORPTION SPECTROSCOPY OF NITROMETHANE PHOTOLYSIS

W. L. FAUST, L. S. GOLDBERG, T. R. ROYT, J. N. BRADFORD,
R. T. WILLIAMS, AND J. M. SCHNUR
Naval Research Laboratory, Washington, D.C. 20375

P. G. STONE AND R. G. WEISS*
Department of Chemistry, Georgetown University
Washington, D.C. 20057

We are applying short pulse techniques to studies of small molecular fragments, stable or reactive radical species emergent as the primary products of unimolecular decomposition of simple photolabile materials. Nitromethane (CH_3NO_2) photolysis has been the subject of extensive prior investigations under varying conditions of irradiation wavelength, phase, temperature, and with active additives. The identity of the primary products and the kinetics of the reaction remain unresolved, although several mechanisms have been advanced to explain the observed products. From nitromethane vapor the list of major final products which have been reported [1] includes CH_3ONO, CH_2O, CH_3NO, NO, and N_2O; minor final products include H_2, CH_4, N_2, and CO; and a number of reaction intermediates have been reported, notably NO_2 and HNO. As an inferred early product, NO_2 was estimated to have a quantum yield as large as 0.6, and this fragment has been our principal object of study to date.

The present experiment employs a short pulse of the Nd 4th harmonic to excite condensed-phase nitromethane on its first electronic transition $n \rightarrow \pi^*$ (λ_{max} = 270 nm). We have recorded an extensive band of absorption which we attribute to the nitro radical NO_2 (Fig. 1). The onset of the absorption is not immediate; it becomes detectable a few nanoseconds after the ultraviolet pulse and is still rising after 13 nanoseconds (Fig. 2). The intensity of the absorption is consistent with a substantial yield.

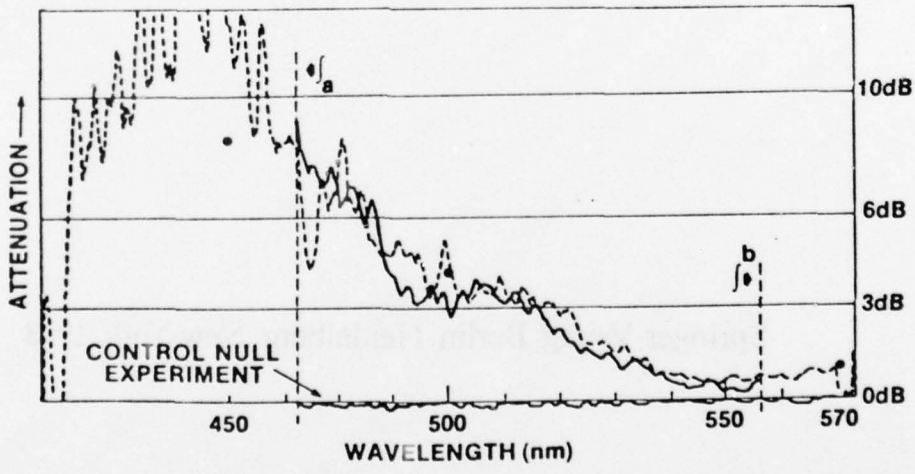

Fig. 1. Spectrum of absorption at 13.9 nsec delay. The relative NO_2 concentration at a given interrogation time was taken by the integration of the attenuation between the limits displayed in the figure, where the detected probe light signal level was adequate. Two shots are displayed.

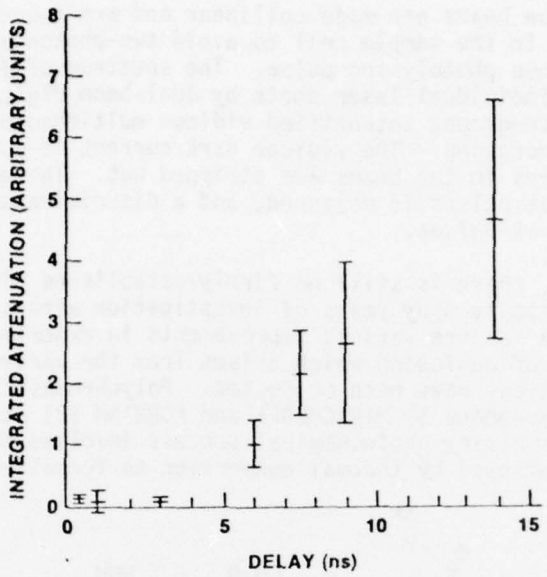

Fig. 2. Temporal development of integrated attenuation attributed to NO_2 absorption, following a photolysis pulse of about 2.5 mj energy.

The detection of NO_2 presents a significant challenge in that its absorption cross section σ is small. Measurements on low pressure NO_2 gas, which absorbs in a very broad band extending roughly from 300 to 550 nm, give $\sigma \sim 3 \times 10^{-18}$ cm^2. Most previous short-pulse continuum studies, in contrast, have dealt with highly-conjugated systems such as polyenes, with cross sections two orders of magnitude larger. We have also sought HNO, which has accessible absorption in the red and which has been considered potentially an important primary product; but no clear indication of this species has been found under the current conditions.

The picosecond photolysis apparatus was constructed with the capability to observe spectra of weakly absorbing transient species. The laser system comprises a passively modelocked Nd:YAG oscillator, a single pulse selector, and a double-pass Nd:YAG amplifier to provide a 1.064 μm pulse of up to 25 mJ energy and 30 ps duration. A frequency doubler and a redoubler, both of KD*P, generate a 266 nm photolysing pulse of 3 to 4 mJ energy. The ultraviolet pulse is brought to a submillimeter diameter focus (~500 μm) in the sample cell (2 mm thick) in order to provide sufficiently high energy density to produce adequate NO_2 for observation. A white light continuum pulse is used to probe this small photolysed region. The residual 1.064 μm light after frequency doubling passes through a variable optical delay and is focused into a 15 cm cell of D_2O. The emergent continuum beam is then steered through the center of a 600 μm pinhole just beyond the D_2O cell and is imaged by a lens to a 350 μm diameter spot in the sample cell. The lens is apertured to pass only a small portion of the central, relatively homogeneous core of the continuum light. A beam splitter is used to divert a replica of the focused probe beam to impinge on a second spot in the sample cell. This provides a reference beam identical to the signal beam with regard to any lateral variation of the spectral distribution. The ultra-

violet and main probe beams are made collinear and are focused independently. LiF windows are used in the sample cell to avoid two-photon absorption and damage from the intense photolysing pulse. The spectrum of induced absorption is measured on individual laser shots by dual-beam digital ratiometry using a grating spectrograph, intensified vidicon multichannel recording, and computer data processing. The vidicon dark current is subtracted and instrumental variations in the beams are stripped out. The energy of the individual ultraviolet pulses is measured, and a discriminator threshold is employed to reject weak pulses.

As we noted above, there is still no firmly-established picture of nitromethane photolysis despite many years of investigation with several experimental approaches and despite various improvements in experimental technique. There is a component of confusion which arises from the varied conditions under which the reactions have been conducted. Polychromatic flash excitation of gaseous nitromethane by HIRSCHLAFF and NORRISH [2] at 101°C led them to conclude that the primary photochemical process involved the formation of the aci from I, followed by thermal conversion to formaldehyde and nitroxyl:

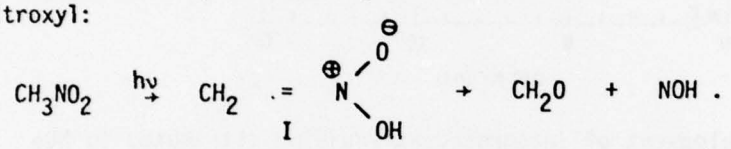

Later NAPIER and NORRISH [3] reexamined the flash photolysis of gaseous nitromethane in the presence of an excess of nitrogen. The results of these experiments indicated that homolytic scission of the carbon-nitrogen bond to form methyl and nitro radicals is the first step:

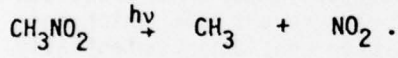

The latter mechanism was favored also by BROWN and PIMENTEL [4] on the basis of low-temperature photolysis work, and later by McGARVEY and McGRATH [5] who again employed flash techniques with gaseous nitromethane. Classical photochemical techniques were applied by HONDA, MIKUNI, and TAKAHASI [1], who concluded that gaseous nitromethane at 55°C under irradiation at 313 nm yields formaldehyde and nitroxyl from the excited singlet state, methyl and nitro from the triplet.

Considering the import of our own measurements, we do not suppose that NO_2 is formed directly from the nitromethane singlet in a process protracted over nanoseconds and with substantial yield, since competing processes of internal conversion and intersystem crossing should dominate this. The long delay which we have found for NO_2 formation is consistent with either a triplet or an isomer such as the aci form I of nitromethane as the precursor. We plan additional tests addressed specifically toward each of these possibilities for the intermediate.

We have found some unexpected but interesting effects associated with relatively high intensities in the probe beam. This beam itself can give rise to new absorption in the red, beyond the NO_2 region. These effects abate for adequately reduced probe intensity levels which still are readily measured with the intensified vidicon. Also, we find no such effects at

small time delays such that the principal NO_2 absorption has not yet developed. It is clear that such investigations must be executed with careful regard for stepwise and nonlinear effects associated with high levels of probing flux. This concern must be heightened for work with still shorter pulses.

Since there is a diversity of potential products in nitromethane photolysis, it was essential to acquire spectral information across as broad a band as possible for the distinct identification of the species present. On the other hand, the KCl F center, for which we give a brief discussion of new results, is a case for which the gross features of the spectroscopy at least were understood at the outset. In this circumstance discrete-frequency synchronous probe beams remain very useful for studies of temporal development and for actinometric measurements. The F center yield following two-quantum excitation possesses an interesting temperature dependence (Fig. 3). It approaches unity near the melting point (1049°C), and absorption persists even into the molten state. It should be appreciated that the stable population of these centers apparent to conventional means of measurement is reduced by two orders of magnitude or more because of very fast annealing of the complementary F and H centers. The temperature dependence then also acquires additional structure.

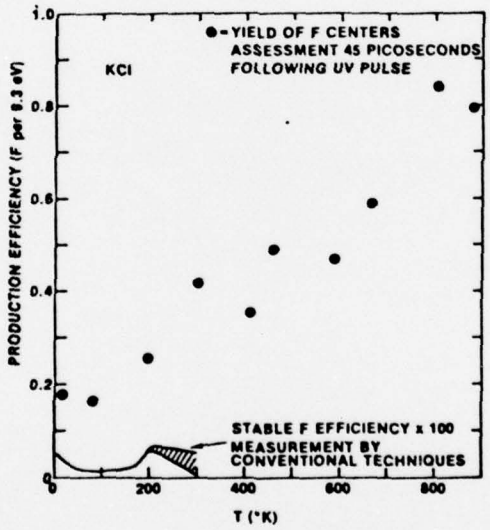

Fig. 3. The yield of F centers per two-photon absorption event as assessed with a 532 nm probe pulse. The production efficiency has been corrected for temperature dependence of the F-band spectrum.

References

*Research supported by the Office of Naval Research.

1. K. Honda, H. Mikuni, and M. Takahasi, Bull. Chem. Soc. Japan 45, 3534 (1972).
2. E. Hirschlaff and R. G. W. Norrish, J. Chem. Soc. 1580 (1936).
3. I. M. Napier and R. G. W. Norrish, Proc. Roy. Soc. A 299, 317 (1967).
4. H. W. Brown and G. C. Pimentel, J. Chem. Phys. 29, 883 (1958).
5. J. J. McGarvey and W. D. McGrath, Trans. Faraday Soc. 60, 2196 (1964).